Chemical Science

Supplementary Information for

Exploiting Single-Electron Transfer in Lewis Pairs for Catalytic Bond-Forming Reactions

Yoshitaka Aramaki,[a] Naoki Imaizumi,[a] Mao Hotta,[a] Jun Kumagai,[b] and Takashi Ooi[a,c]

[a] *Institute of Transformative Bio-Molecules (WPI-ITbM) and Department of Molecular and Macromolecular Chemistry, Graduate School of Engineering, Nagoya University, Nagoya 464-8601, Japan*
[b] *Institute of Materials and Systems for Sustainability, Nagoya University, Nagoya 464-8601, Japan*
[c] *CREST, Japan Science and Technology Agency (JST), Nagoya University, Nagoya 464-8601, Japan*

tooi@chembio.nagoya-u.ac.jp

Contents

I. General information

Infrared spectra were recorded on a Shimadzu IRAffinity-1 spectrometer. ^{1}H NMR spectra were recorded on JEOL JNM-ECS400 (400 MHz), JEOL JNM-ECA500II (500 MHz), and JEOL JNM-ECA600II (600 MHz) spectrometers. Chemical shifts are reported in ppm from the solvent resonance (CD_2Cl_2; 5.32 ppm, CD_3CN; 1.94 ppm, THF-d_8; 3.58 ppm) or the tetramethylsilane resonance (0.00 ppm) as the internal standard ($CDCl_3$). Data are reported as follows: chemical shift, multiplicity (s = singlet, d = doublet, t = triplet, q = quartet, m = multiplet, and br = broad), coupling constants (Hz), and integration. $^{13}C\{^{1}H\}$ NMR spectra were recorded on a JEOL JNM-ECA600II (151 MHz) spectrometer with complete proton decoupling. Chemical shifts are reported in ppm from the solvent resonance as the internal standard ($CDCl_3$; 77.16 ppm). ^{11}B NMR spectra were recorded on JEOL-ECS400 (128 MHz) and JNM-ECA500II (161 MHz) spectrometers. Chemical shift are reported in ppm from $BF_3{\cdot}OEt_2$ resonance (0.0 ppm) as an external standard. CD_3CN was dried over CaH_2 under reflux condition and distilled prior to use. The high resolution mass spectra were conducted on a Thermo Fisher Scientific Exactive (ESI). Analytical thin layer chromatography (TLC) was performed on Merck precoated TLC plates (silica gel 60 GF254, 0.25 mm). Flash column chromatography was performed on silica gel 60 (spherical, 40-50 μm; Kanto Chemical Co., Inc.), silica gel 60 (Merck 1.09385.9929, 230-400 mesh), CHROMATOREX DIOL MB100-40/75 (spherical, 40~75 μm; Fuji Silysia Chemical ltd.), CHROMATOREX NH DM2035 (spherical, 60 μm; Fuji Silysia Chemical ltd.), and CHROMATOREX COOH MB100-40/75 (spherical, 40~75 μm; Fuji Silysia Chemical ltd.). Recycling preparative HPLC was performed using YMC HPLC LC forte/R or JAI LaboAce LC5060 equipped with silica gel column (ϕ20 mm × 250 mm, YMC-Pack SIL SL 12S05-2520WT).

All air- and moisture-sensitive reactions were performed under an atmosphere of argon (Ar) in dried glassware. Dichloromethane (CH_2Cl_2), 1,2-dichloroethane (DCE), and acetonitrile (MeCN) were supplied from Kanto Chemical Co., Inc. as "Dehydrated" and further purified by both A2 alumina and Q5 reactant using a GlassContour solvent dispensing system. Other simple chemicals were purchased and used as such.

All experiments involving light irradiation were performed with 405 nm LEDs light (CCS inc., Model:HLV-24VL405-4WHI, irradiance: ~1000 W/m^2 at 0 mm from the light).

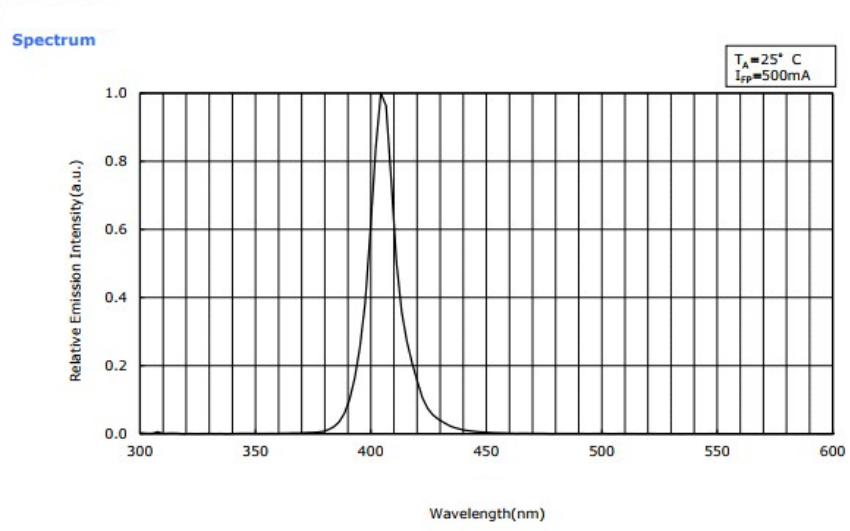

Fig. S1 Emission spectrum of 405 nm LED element (provided from CCS inc).

II. UV-vis absorption spectroscopy

$B(C_6F_5)_3$ and *p*-bromo-*N*,*N*-dimethylaniline (**2**) were sublimated, and *p*-bromo-*N*-methyl-*N*-($TMSCH_2$)aniline (**1a**), *N*-aryltetrahydroisoquinolines (**5a**, **5b**, and **5d**) were distilled or sublimated before sample preparation. All sample solutions were prepared in an argon-filled glovebox with dehydrated solvent from the solvent dispensing system, which were further degassed by freeze-pump-thaw cycle three times. The sample solutions were transferred into screw-capped quartz cells sealed with Teflon tape to avoid contamination of water and oxygen. All spectra were recorded on a SHIMADZU UV-1800 spectrophotometer.

UV-vis absorption spectra of $B(C_6F_5)_3$, **1a**, and **2**

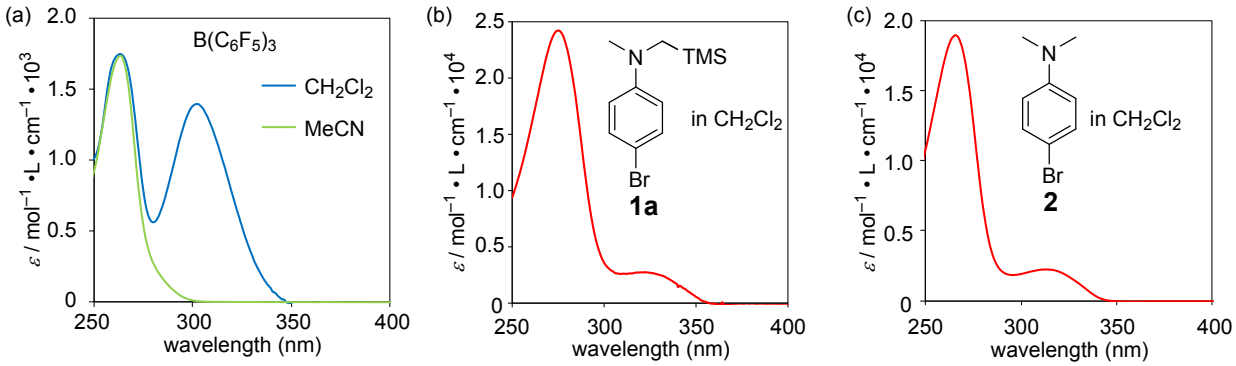

Fig. S2 UV-vis absorption spectra of (a) $B(C_6F_5)_3$ in CH_2Cl_2 (blue) and MeCN (green); (b) **1a** in CH_2Cl_2; (c) **2** in CH_2Cl_2. The difference in the absorption spectra of $B(C_6F_5)_3$ recorded in MeCN and CH_2Cl_2 is probably due to the coordination of MeCN to $B(C_6F_5)_3$ as detected by ^{11}B NMR spectroscopy (see Fig. S20).

Oxidation of **1a** by $AgBAr^f$ and **2** by $AgSbF_6$

$AgBAr^f$ was prepared by following the literature procedure.[1] Compound **1a** (0.10 mmol) and $AgBAr^f$ (0.10 mmol), or **2** (0.10 mmol) and $AgSbF_6$ (34 mg, 0.10 mmol) were added to a test tube. Argon gas was purged and the test tube was capped with a rubber septum. After addition of 1 mL of CH_2Cl_2, the mixture was stirred at room temperature. During the stirring, the solution turned from colorless to blue-green. After 1 h (for **1a**) or 2 h (for **2**) of stirring, the solution was passed through a membrane filter to remove the precipitates. 100 μL of the filtrate was diluted into 10 mL with CH_2Cl_2 and an absorption spectra were recorded.

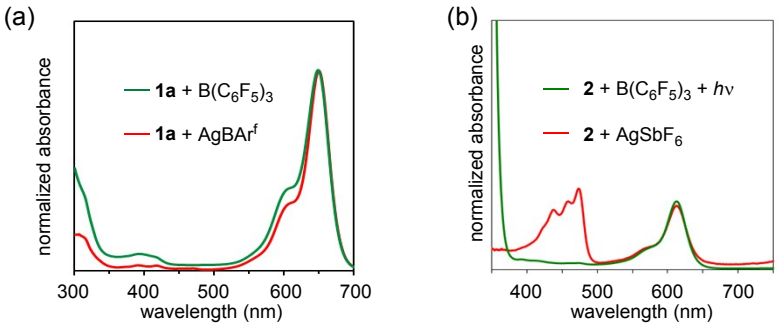

Fig S3 (a) The absorption spectrum of $B(C_6F_5)$ and **1a** after 1 h of stirring (green) in comparison with that of a mixture of $AgBAr^f$ and **1a** (red). (b) The absorption spectrum of $B(C_6F_5)_3$ and **2** after 405 nm LED irradiation for 3 h (green) in comparison with that of $AgSbF_6$ and **2** after 2 h of stirring (red).

[1] (a) Y. Hayashi, J. J. Rohde, E. J. Corey, *J. Am. Chem. Soc.*, 1996, **118**, 5502; (b) O. Shyshov, R. Brachvogel, T. Bachmann, R. Srikantharajah, D. Segets, F. Hampel, R. Puchta, M. von Deius, *Angew. Chem. Int. Ed.*, 2017, **56**, 776.

UV-vis spectra of *N*-aryltetrahydroisoquinolines (**5a**, **5b**, and **5d**) in the presence and absence of $B(C_6F_5)_3$ in MeCN

Longer-wavelength shifts of absorption peaks were also observed with **5a** and **5b** in the presence of $B(C_6F_5)_3$ in MeCN, suggesting the formation of EDA complexes (Fig. S4a and b). On the other hand, longer-wavelength shift was not observed with *ortho*-tolyltetrahydroisoquinoline (**5d**) (Fig. S4c), and thus no EDA complex formed probably because of the steric hindrance. This result was consistent with the fact that bond formation did not occur in the reaction of **5d** with **3a** in the presence of 10 mol% of $B(C_6F_5)_3$ in MeCN under 405 nm LED irradiation (Table 2, entry 8).

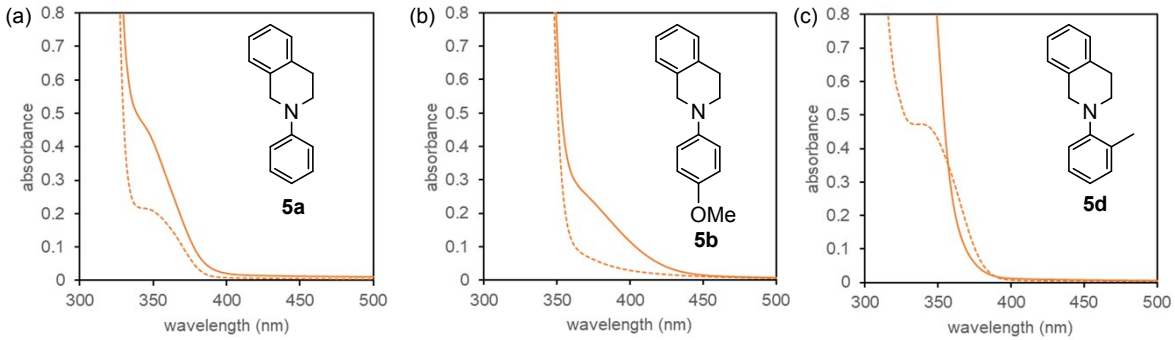

Fig. S4 The absorption spectra of *N*-aryltetrahydroisoquinolines (**5a**, **5b**, and **5d**, $1.0 \cdot 10^{-2}$ M, hashed line) and those in the presence of $B(C_6F_5)_3$ ($1.0 \cdot 10^{-2}$ M, solid line) in MeCN.

Methyl vinyl ketone (**3a**) in the presence and absence of $B(C_6F_5)_3$ in MeCN

Methyl vinyl ketone (**3a**) itself and the mixture with $B(C_6F_5)_3$ did not absorb over 380 nm of light (Fig. S5), indicating that methyl vinyl ketone was not excited by 405 nm LED irradiation (Fig. S1) even in the presence of $B(C_6F_5)_3$.

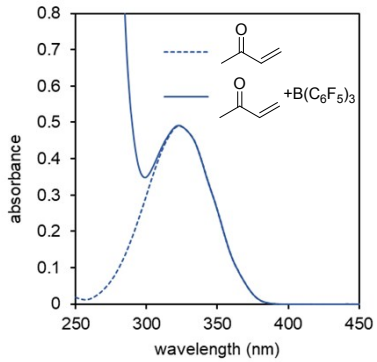

Fig. S5 Absorption spectra of methyl vinyl ketone **3a** (hashed line, $1.1 \cdot 10^{-2}$ M) and that in the presence of $B(C_6F_5)_3$ (solid line, $1.1 \cdot 10^{-2}$ M) in MeCN.

III. ESR spectroscopy

All ESR spectra were recorded on an *X*-band ESR spectrometer (JEOL JES-RE1X) at room temperature. *p*-Bromo-*N*-methyl-*N*-(TMSCH_2)aniline (**1a**) was distilled, *p*-bromo-*N*,*N*-dimethylaniline **2** and B(C_6F_5)$_3$ were sublimated, and CH_2Cl_2 from the solvent dispensing system was further degassed by freeze-pump-thaw cycle three times. The sample solution was prepared in an argon-purged glovebox and transferred into a screw-capped ESR sample tube (3ϕ) sealed with Teflon tape in order to avoid contamination of oxygen and water. The samples were set to the center of an ESR cavity equipped with collecting lens, and the light irradiation experiment was performed using 405 nm LED through the lens. Typical ESR parameters for the measurements were microwave power of 4.0 mW, field modulation width of 0.05 mT at 100 kHz, static magnetic field of 325.5 ± 5 mT. Microwave frequency and magnetic field of the spectrometer were monitored using a microwave frequency counter (Hewlett-Packard, 53150A) and an NMR field meter (Echo Electronics Co. Ltd., EFM-2000AX), respectively. For precise assignment of *g*-values, a center peak of ca. 0.1 mM of perylene (Sigma Aldrich 99+%) radical cation in concentrated H_2SO_4 (Kanto Chemical, > 95%), which shows the center peak at apparent *g*-value of 2.002583 with very narrow maximum slope line width (ΔH_{msl} ~ 0.01 mT), was used for the correction of the NMR field meter.[2,3] ESR parameters for the simulation of ESR spectra were optimized with EasySpin software.[4] The sample of [**2**$^{\bullet}$]$^+$[SbF_6]$^-$ was prepared as described in that for the absorption spectrum measurement (see page S3). No observable decay of the signal was detected for [**2**$^{\bullet}$]$^+$[SbF_6]$^-$ during 48 min monitoring (Fig. S7(c)).

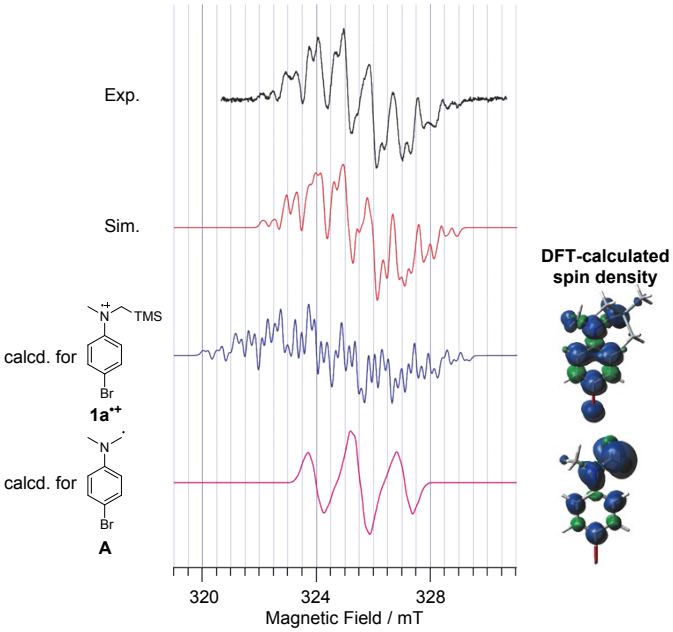

Fig. S6 ESR spectra of the mixture of B(C_6F_5)$_3$ and **1a** in CH_2Cl_2, simulated spectrum (see Table S1 for the ESR parameters for the simulation), DFT-calculated spectrum for **1a**$^{\bullet+}$, and DFT-calculated spectrum of radical **A** with visualized spin density of **1a**$^{\bullet+}$ and **A** (isovalue = 0.001). See also VI computational studies section for the details of DFT calculations.

[2] J. Kumagai, M. Hanabusa, H. Inagaki, S. Kariya, *Phys. Chem. Chem. Phys.*, 2004, **6**, 4363.

[3] B. G. Segal, M. Kaplan, G. K. Fraenkel, *J. Chem. Phys.*, 1965, **43**, 4191.

[4] S. Stoll, A. Schweiger, *J. Magn. Reson.*, 2006, **178**, 42.

Table S1 Isotropic hyperfine coupling constants (HFCC) and *g* values for simulated ESR spectrum in Fig. S6 and comparison with calculated HFCC values of **1a**$^{\bullet+}$ and radical **A**

Nuclei in the molecules	HFCC / MHz		
	Simulated [a]	Calculated [b]	
		1a$^{\bullet+}$	radical **A**
N	23.1	22.1	2.68
3H in CH_3-	20.7	32.4	6.12
1H in -CH_2	27.8	39.8	-46.5
1H in -CH_2	26.2	24.6	-40.8
2H in ortho position	9.68	–12.1	-4.94
2H in meta position	3.73	4.50	2.0
^{29}Si	8.78	-24.1	-
g value	2.0033	2.0084	2.0032

[a)] HFCC in absolute value

[b)] UB3LYP/6-311+G(d, p) level with PCM = dichloromethane option

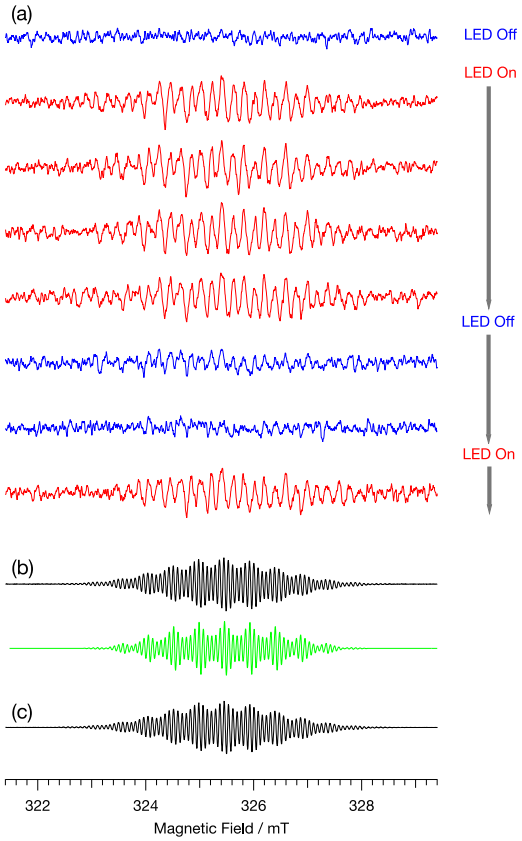

Fig. S7 (a) 405 nm LED light on/off experiments of $B(C_6F_5)_3$ and **2** in CH_2Cl_2 ($1.0 \cdot 10^{-2}$ M, respectively). The intervals of each measurements are 9 min. (b) $[\mathbf{2}^{\bullet}]^+[SbF_6]^-$ in CH_2Cl_2 with a simulated spectrum (green). (c) 48 min after the measurement of Fig. S7b. Spectra positions are corrected to the microwave frequency of 9.1240 GHz.

Table S2 Isotropic hyperfine coupling constants (A) of $\mathbf{2}^{\bullet+}$ with different pairing anions

pairing anion	A / MHz			
	N	CH_3	*ortho*-H	*meta*-H
$B(C_6F_5)_3^{\bullet-}$	32.91	21.66	11.61	5.75
SbF_6^-	26.38	13.18	4.48	2.21

IV. Electrochemical analysis

Cyclic voltammetry (CV) and square wave voltammetry (SWV) were performed with a ALS/chi-617A Potentiostat/Galvanostat interfaced to a base PC using the EG&G Model 270 software package. The cell was a standard three electrode setup using a 3 mm diameter glassy carbon working electrode, a platinum wire counter electrode, and a reference electrode consisting of a silver wire in a glass tube containing a 0.1 M solution of tetrabutylammonium perchlorate (TBAP) in MeCN.

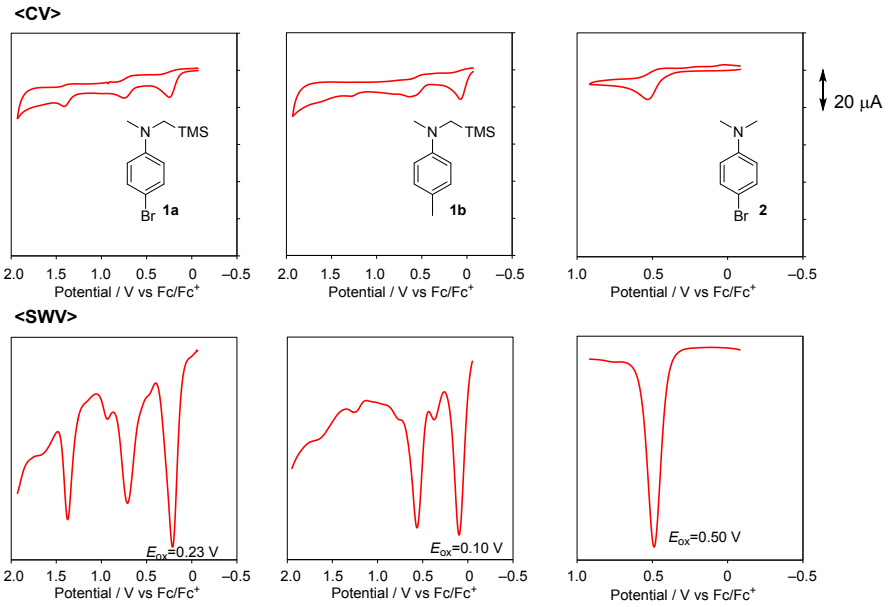

Fig. S8 Cyclic voltammogram (upper) and square wave voltammogram (bottom) of **1a**, **1b**, and **2**.

V. Crystallographic structure determination

A suitable single co-crystal of $B(C_6F_5)_3$ and **2** was mounted with fluorine oil on MicroMounts. Data of X-ray diffraction were collected at 123 K on a Rigaku FR-X with Pilatus 200K with fine-focus sealed tube Mo/Kα radiation (λ = 0.71075 Å). The structure was solved by direct method with SIR-97[5] and refined by a full-matrix least square method on F^2 for all reflections (SHELXL-2014).[6] All non-hydrogen atoms were refined with anisotropic displacement parameters. All hydrogen atoms were placed using AFIX instruction.

Table S3 Crystal data and structure refinement for co-crystal of $B(C_6F_5)_3$ and **2**

	$B(C_6F_5)_3$ and **2**
formula	$C_{26}H_{10}BBrF_{15}N$
formula weight	712.07
T (K)	123(2)
λ (Å)	0.71075
cryst syst	*Triclinic*
space group	$P\bar{1}$
a, (Å)	7.300(5)
b, (Å)	11.867(8)
c, (Å)	15.598(9)
α,(°)	78.16(4)
β, (°)	80.45(4)
γ, (°)	88.78(5)
volume, (Å^3)	1304.1(15)
Z	2
D_{calc}, (g / cm^3)	1.813
μ (mm^{-1})	1.703
F(000)	696
cryst size (mm)	0.10 × 0.05 × 0.02
2θ range, (deg)	3.288−27.497
Index ranges	-9<=h<=9 -18<=k<=15 -18<=l<=20
reflns collected	9948
indep reflns/R_{int}	5538/0.0591
params	399
GOF on F^2	0.834
R_1, wR_2 [I>2σ(I)]	0.0518, 0.1073
R_1, wR_2 (all data)	0.1239, 0.1267
Peak and hole (e.Å^{-3})	0.518, -0.464

[5] A. Altomare, M. C. Burla, M. Camalli, G. L. Cascarano, C. Giacovazzo, A. Guagliardi, A. G. G. Moliterni, G. Polidori, R. Spagna, *J. Appl. Crystallogr.*, 1999, **32**, 115.
[6] G. M. Sheldrick, *Act. Cryst.*, 2015, **C71**, 3.

Table S4 Selected bond lengths and dihedral angles of **2** in co-crystal with $B(C_6F_5)_3$

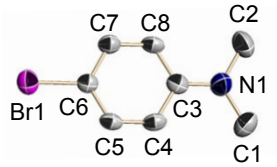

	Bond Length (Å)
N1–C1	1.451(6)
N1–C2	1.447(6)
N1–C3	1.366(6)
C3–C4	1.402(6)
C4–C5	1.372(6)
C5–C6	1.380(6)
C6–C7	1.400(6)
C7–C8	1.368(6)
C3–C8	1.422(6)
C6–Br1	1.883(4)
	Bond Angle (°)
C2–N1–C1	119.2(4)
C3–N1–C1	120.5(4)
C3–N1–C2	120.2(4)
	Dihedral Angle (°)
C2–N1–C3–C4	178.5(5)
C1–N1–C3–C4	−4.4(7)
C2–N1–C3–C8	−0.7(7)
C1–N1–C3–C8	176.3(4)

VI. Computational studies

All theoretical calculations were performed with density functional theory (DFT)[7] method using Gaussian 09 program (Revision D.01)[8] and the results were produced with Gauss View 5.0.9.[9] For time-dependent DFT (TD-DFT) calculations[10] of *anti*-complex of $B(C_6F_5)_3$ and **2**, the X-ray structure of the co-crystal was used without further geometry optimization. For the other structures, TD-DFT calculations were performed for geometry-optimized structures.

Calculation for the Gibbs free energy difference between neutral states and radical cations of **1a** and **2**

The structures optimization and frequency calculations of **1a**, $\mathbf{1a}^{\bullet+}$, **2**, and $\mathbf{2}^{\bullet+}$ were calculated at (U)B3LYP/6-311+G(d,p) level with using PCM solvation model[11] (solvent = dichloromethane). The calculated Gibbs free energies were as following; −3348.378363 (**1a**), −3348.1185352 ($\mathbf{1a}^{\bullet+}$), −2939.736115 (**2**), and −2939.536346 ($\mathbf{2}^{\bullet+}$) (Hartree).

TD-DFT calculations for *syn*-complex, and Lewis adduct of $B(C_6F_5)_3$ and **2**

Although *anti*-complex structure was obtained from X-ray crystallography, the other conformation, *syn*-complex, and Lewis adduct should be considered in solution. Therefore, the lowest transitions for these structures were calculated by TD-DFT calculations at CAM-B3LYP[12]/6-311+G(d,p) level for geometry-optimized structures. In the optimized structure of the Lewis adduct, B–N bond length (1.88 Å) was longer than that of BH_3•NH_3 (1.66 Å),[13] suggesting that the Lewis adduct structure was relatively unstable due to the steric repulsion. In addition, the lowest transition energy of the Lewis adduct structure was calculated to be 5.15 eV corresponding to 241 nm of wavelength and the excitation had local excitation character (π-π* excitation of a bromophenyl moiety of **2** and a C_6F_5 moiety of $B(C_6F_5)_3$) rather than charge-transfer (CT) character (Fig. S10). Therefore, the contribution of the Lewis adduct to the SET reaction can be ruled out.

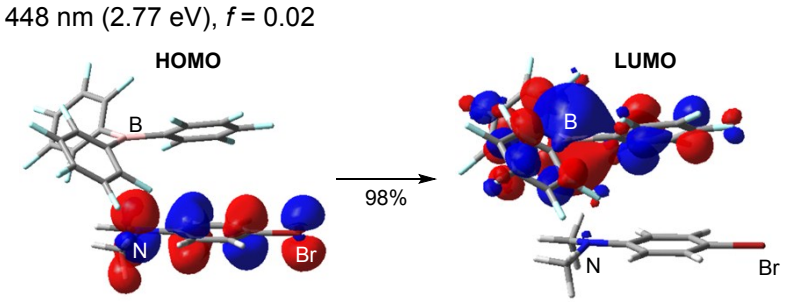

Fig. S9 The TD-DFT-calculated lowest transition (HOMO to LUMO) for *syn*-complex of $B(C_6F_5)_3$ and **2**.

---

[7] R. G. Parr, W. Yang, *Density-Functional Theory of Atoms and Molecules* Oxford University Press, New York, 1989.
[8] M. J. Frisch, G. W. Trucks, H. B. Schlegel, G. E. Scuseria, M. A. Robb, J. R. Cheeseman, G. Scalmani, V. Barone, B. Mennucci, G. A. Petersson, H. Nakatsuji, M. Caricato, X. Li, H. P. Hratchian, A. F. Izmaylov, J. Bloino, G. Zheng, J. L. Sonnenberg, M. Hada, M. Ehara, K. Toyota, R. Fukuda, J. Hasegawa, M. Ishida, T. Nakajima, Y. Honda, O. Kitao, H. Nakai, T. Vreven, J. Montgomery, J. A., J. E. Peralta, F. Ogliaro, M. Bearpark, J. J. Heyd, E. Brothers, K. N. Kudin, V. N. Staroverov, T. Keith, R. Kobayashi, J. Normand, K. Raghavachari, A. Rendell, J. C. Burant, S. S. Iyengar, J. Tomasi, M. Cossi, N. Rega, J. M. Millam, M. Klene, J. E. Knox, J. B. Cross, V. Bakken, C. Adamo, J. Jaramillo, R. Gomperts, R. E. Stratmann, O. Yazyev, A. J. Austin, R. Cammi, C. Pomelli, J. W. Ochterski, R. L. Martin, K. Morokuma, V. G. Zakrzewski, G. A. Voth, P. Salvador, J. J. Dannenberg, S. Dapprich, A. D. Daniels, Ö. Farkas, J. B. Foresman, J. V. Ortiz, J. Cioslowski, Gaussian, Inc.: Wallingford CT, 2013.
[9] R. Dennington, T. A. Keith, J. M. Millam, Semichem inc., Shawnee Mission, KS, 2008
[10] E. Runge, E. K. U. Gross, *Phys. Rev. Lett.,* 1984, **52**, 997.
[11] J. Tomasi, B. Mennucci, R. Cammi, *Chem. Rev.*, 2005, **105**, 2999.
[12] T. Yanai, D. P. Tew, N. C. Handy, *Chem. Phys. Lett.*, 2004, **393**, 51.
[13] L. R. Thorne, *J. Chem. Phys.* 1983, **78**, 167.

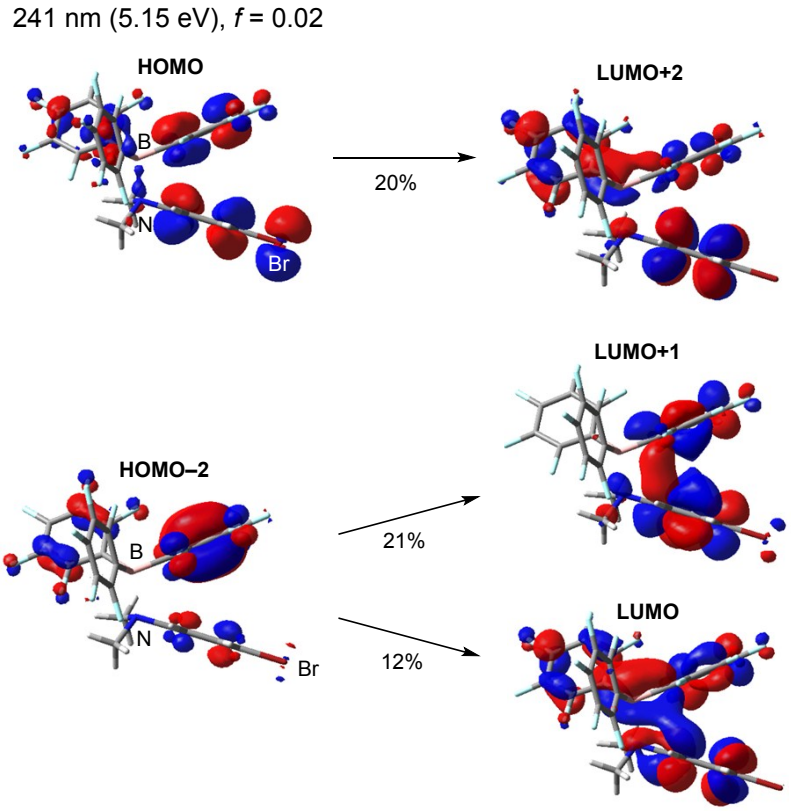

Fig. S10 The TD-DFT-calculated lowest transition for Lewis adduct of $B(C_6F_5)_3$ and **2**.

TD-DFT calculations for EDA complexes and Lewis adduct of $B(C_6F_5)_3$ and *N*-phenyltetrahydroisoquinoline (**5a**)

For *syn*-complex and B–N Lewis adduct, both geometry optimizations and TD-DFT calculations were performed at CAM-B3LYP/6-311+G(d,p) level. For *anti*-complex, the geometry was optimized at B3LYP/6-31G(d) level and TD-DFT calculation was performed at CAM-B3LYP/6-311+G(d,p) level. For all three structures, TD-DFT calculations were performed using PCM solvation model[14] (solvent = acetonitrile). As revealed in the calculations for those of **2**, both *syn*-complex and *anti*-complex showed charge-transfer character with ca. 440 nm of wavelength (Fig. S11 and S12), while the Lewis adduct showed local excitation character with 237 nm of wavelength (Fig. S13).

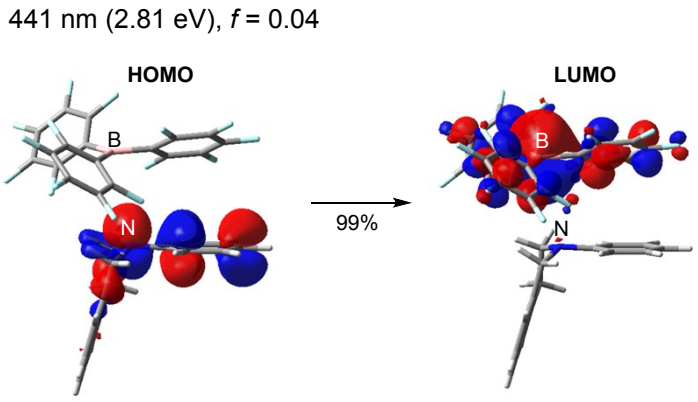

Fig. S11 The TD-DFT-calculated lowest transition (HOMO to LUMO) for *syn*-complex of $B(C_6F_5)_3$ and **5a**.

[14] J. Tomasi, B. Mennucci, R. Cammi, *Chem. Rev.*, 2005, **105**, 2999.

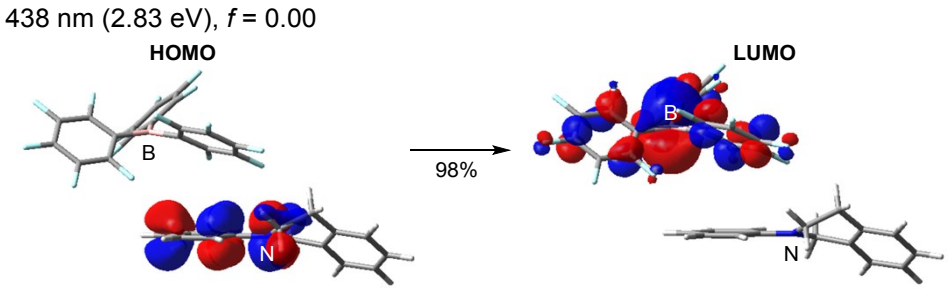

Fig. S12 The TD-DFT-calculated lowest transition (HOMO to LUMO) for *anti*-complex of $B(C_6F_5)_3$ and **5a**.

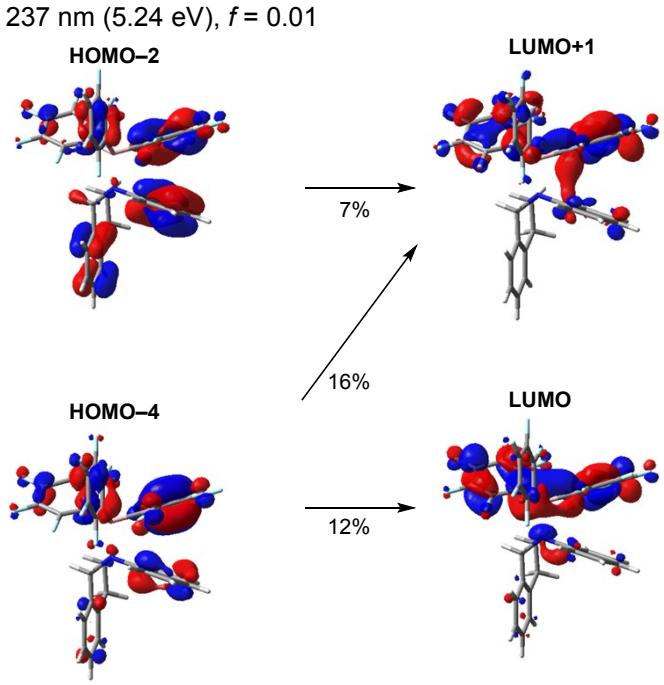

Fig. S13 The TD-DFT-calculated lowest transition for the Lewis adduct of $B(C_6F_5)_3$ and **5a**.

Cartesian coordination of 1a

C	-0.29660000	-0.50057000	-0.56540100
C	0.11688900	0.82283600	-0.27457500
C	-0.89224000	1.73105300	0.13329900
C	-2.22183100	1.33896000	0.24673000
C	-2.58839700	0.03086900	-0.04784100
C	-1.62692400	-0.88809800	-0.45494600
H	0.42374900	-1.24783500	-0.86406800
H	-0.64708900	2.75882100	0.35992600
H	-2.96420300	2.06272400	0.55962200
H	-1.90296800	-1.91044700	-0.68204300
N	1.43369600	1.21605500	-0.36900500
C	1.79489000	2.59950900	-0.09378600
H	2.87841500	2.69409700	-0.12125800
H	1.37017500	3.29441000	-0.83211700
H	1.46204600	2.90815600	0.90093100
C	2.45306900	0.38750700	-1.03574000
H	3.08609200	1.05455400	-1.63232500
H	1.97684400	-0.27249600	-1.76680600
Si	3.60293300	-0.62804900	0.12368300
C	4.91358100	-1.43556300	-0.97190600
H	5.61195200	-2.02632000	-0.37076900
H	4.46095700	-2.10614300	-1.70903900
H	5.49592500	-0.68438000	-1.51444200
C	4.42409400	0.53364600	1.36613800
H	5.03108000	1.29535700	0.86722200
H	3.68152500	1.04500800	1.98578900
H	5.08209100	-0.02989200	2.03537100
C	2.63595500	-1.95445400	1.05616000
H	1.82564600	-1.52257700	1.65020200
H	2.19989200	-2.68974700	0.37359800
H	3.30147100	-2.49094400	1.74046600
Br	-4.43215600	-0.50989200	0.10635500

Cartesian coordination of $1a^{\bullet+}$

C	-0.85316000	1.70939300	0.16420400
C	-2.16912500	1.32642800	0.31109200
C	-2.56123800	0.03359100	-0.05826900
C	-1.63107300	-0.87691400	-0.57683000
C	-0.31493500	-0.49848700	-0.73157200
C	0.11341600	0.80824600	-0.36550100
H	-0.57683500	2.71266600	0.45139000
H	-2.89185800	2.02587700	0.70887000
Br	-4.36993900	-0.48823700	0.14132800
H	-1.94047300	-1.87460500	-0.85753600
H	0.37904500	-1.22155000	-1.13124500
N	1.41422700	1.20519200	-0.52171200
C	1.83103700	2.55574000	-0.11167700
C	2.44877700	0.36532600	-1.08449400
H	1.57082000	2.73856100	0.93043000
H	2.90617500	2.63903100	-0.22917900
H	1.34596400	3.29996000	-0.74675400
H	2.02761400	-0.35149100	-1.78653400
H	3.13409900	1.00918100	-1.63898300
Si	3.56540000	-0.63927100	0.19430900
C	4.32744900	0.55178400	1.43140200
C	2.50162100	-1.92595400	1.05719400
C	4.86791000	-1.43400800	-0.90126200
H	4.93782900	1.31569700	0.94207700
H	3.57480700	1.05020300	2.04803600
H	4.98152100	-0.00961100	2.10647200
H	2.08146100	-2.64687700	0.35057400
H	3.12578800	-2.48253500	1.76403700
H	1.68145900	-1.47950000	1.62566700
H	5.52625000	-2.06075200	-0.29173400
H	4.41665500	-2.06996500	-1.66763600
H	5.48827100	-0.68343200	-1.39849600

Cartesian coordination of 2

C	1.00681800	1.20823000	0.00010600
C	1.74520900	0.00004100	-0.00005200
C	1.00684900	-1.20815600	-0.00016100
C	-0.38379600	-1.20599300	-0.00014100
C	-1.07625400	0.00001400	-0.00001000
C	-0.38382700	1.20603700	0.00011600
H	1.51601900	2.16173500	0.00025000
H	1.51608600	-2.16164700	-0.00029000
H	-0.91774000	-2.14819900	-0.00023800
H	-0.91779500	2.14822900	0.00024100
Br	-3.00374500	-0.00001000	0.00001300
N	3.12132900	0.00000100	-0.00010500
C	3.85343900	-1.25795800	0.00028900
H	4.92097700	-1.04806700	0.00060400
H	3.62732700	-1.86068200	0.88804900
H	3.62789500	-1.86094200	-0.88744400
C	3.85359300	1.25787600	-0.00018100
H	4.92110400	1.04784600	-0.00077200
H	3.62740600	1.86091500	-0.88770200
H	3.62829600	1.86060700	0.88779200

Cartesian coordination of $2^{\bullet+}$

C	0.98687100	1.22794400	0.00026300
C	1.71855700	0.00001600	0.00000100
C	0.98688300	-1.22791600	-0.00025500
C	-0.38712800	-1.22316300	-0.00029700
C	-1.07998400	0.00000500	-0.00001300
C	-0.38714000	1.22317900	0.00028900
H	1.50450600	2.17543200	0.00057800
H	1.50453200	-2.17539900	-0.00054000
H	-0.93173600	-2.15758700	-0.00056800
H	-0.93175700	2.15759800	0.00056300
Br	-2.96494200	-0.00000400	-0.00003300

N	3.07178100	0.00000100	0.00000800
C	3.82951100	-1.25974200	0.00063000
H	4.88998100	-1.03239600	0.00158600
H	3.58969200	-1.84272000	0.89171600
H	3.59125700	-1.84267200	-0.89092100
C	3.82957400	1.25971000	-0.00051400
H	4.89003000	1.03230600	-0.00178700
H	3.58957400	1.84291100	-0.89140100
H	3.59157400	1.84244400	0.89123700

Cartesian coordination of *anti*-complex of $B(C_6F_5)_3$ and 2

C	1.85560000	3.47950000	3.82590000
H	2.81740000	3.40540000	3.99910000
H	1.70760000	3.63210000	2.86980000
H	1.40960000	2.64990000	4.09690000
N	1.31190000	4.59170000	4.58330000
C	0.80750000	5.74740000	3.87410000
H	-0.12420000	5.90680000	4.13160000
H	0.85640000	5.58610000	2.90890000
H	1.34870000	6.53200000	4.10290000
C	1.32920000	4.57450000	5.94890000
C	1.78150000	3.46230000	6.67310000
H	2.09270000	2.69910000	6.20030000
C	1.78740000	3.44510000	8.04480000
H	2.10290000	2.67440000	8.50100000
C	1.34420000	4.52990000	8.77350000
C	0.89450000	5.66460000	8.08840000
H	0.60160000	6.42700000	8.57480000
C	0.87540000	5.67910000	6.72130000
H	0.54810000	6.45020000	6.27260000
Br	1.35880000	4.51920000	10.65620000
B	4.94720000	4.52200000	11.18860000
C	4.97210000	4.52490000	9.64080000
C	5.49270000	3.48570000	8.85780000
C	5.49320000	3.47170000	7.48470000
C	5.00110000	4.57170000	6.80410000
C	4.48370000	5.61770000	7.51780000
C	4.47400000	5.59790000	8.88800000
F	6.03270000	2.39800000	9.44410000
F	5.99170000	2.42760000	6.79760000
F	4.99790000	4.57650000	5.47580000
F	3.99360000	6.69200000	6.85610000
F	3.91910000	6.66200000	9.50650000
C	4.75560000	5.80800000	12.07390000
C	5.48070000	6.96380000	11.89330000
C	5.41540000	8.04790000	12.76050000
C	4.55760000	8.00530000	13.83410000
C	3.79360000	6.88770000	14.03880000
C	3.90230000	5.80770000	13.16860000
F	6.34980000	7.06810000	10.87050000
F	6.17310000	9.13930000	12.55580000
F	4.48210000	9.03260000	14.69080000
F	2.95750000	6.81670000	15.08440000
F	3.13640000	4.73270000	13.41790000
C	5.19650000	3.16580000	12.00020000
C	6.15940000	3.09240000	12.97730000
C	6.41140000	1.95200000	13.70310000
C	5.64280000	0.85210000	13.52090000
C	4.64720000	0.84780000	12.56330000
C	4.45460000	2.00100000	11.81950000
F	6.92160000	4.18940000	13.24810000
F	7.41500000	1.93300000	14.59430000
F	5.86670000	-0.25980000	14.24090000
F	3.89600000	-0.23710000	12.37370000
F	3.50750000	1.94700000	10.87420000

Optimized Cartesian coordination of *syn*-complex of $B(C_6F_5)_3$ and 2

C	-0.05302900	0.81313000	-3.40429300
H	0.98522500	0.59951800	-3.65221500
H	-0.06241300	1.71378400	-2.79354100
C	-0.15142000	-1.61491200	-3.15615100
H	0.89516200	-1.53497700	-3.44526400
H	-0.22052000	-2.36425800	-2.36755500
C	-1.91719500	-0.22297600	-2.21596000
C	-2.51112100	1.02431700	-1.96291000
C	-2.69215100	-1.36465900	-1.96259900
C	-3.79451100	1.12153900	-1.45376700
H	-1.97021900	1.93939200	-2.15028900
C	-3.97849300	-1.26658600	-1.45342700
H	-2.30057400	-2.35157000	-2.15776400
C	-4.52778600	-0.02468300	-1.19265100
H	-4.22258700	2.09738000	-1.26451200
H	-4.54849200	-2.16657900	-1.26364300
C	-0.04439200	-0.08925400	1.29255900
C	-0.59111600	0.87499900	2.14207700
C	-0.85146500	-1.20693600	1.06723300
C	-1.83627600	0.75065400	2.72350300
C	-2.10392500	-1.36075700	1.62540400
C	-2.59998800	-0.37311300	2.45817500
C	2.00900200	1.46049200	0.37548600
C	3.36216900	1.70515500	0.59723000
C	1.28191100	2.53612600	-0.12623500
C	3.95822500	2.92727000	0.34948400
C	1.84689300	3.76328000	-0.40824900
C	3.19514900	3.96070500	-0.16342700
C	2.21710800	-1.21789800	0.30353800
C	2.36437500	-2.27997100	1.18823200
C	2.89098100	-1.34127900	-0.90491200
C	3.13452500	-3.39118900	0.90616900
C	3.65114200	-2.44685300	-1.23300700
C	3.77769800	-3.47605100	-0.31676600
N	-0.60206300	-0.32026200	-2.67555900

B	1.36865400	0.05599200	0.65475600
F	3.25971200	-4.37595800	1.78929700
F	1.76251300	-2.24190100	2.38181700
F	4.51053500	-4.53952600	-0.60959000
F	4.25893700	-2.52952400	-2.41330400
F	2.79834100	-0.37230200	-1.82695000
F	4.14710500	0.74647400	1.10048700
F	-0.02398800	2.40150200	-0.37999300
F	1.11226300	4.75234500	-0.90808400
F	3.75074800	5.13441000	-0.41812400
F	5.25008400	3.11651400	0.59570600
F	-0.43224800	-2.19427500	0.27063700
F	0.10446300	1.97149100	2.45600900
F	-2.30523000	1.69252200	3.53498500
F	-3.79248300	-0.50749000	3.00906800
F	-2.82865700	-2.44666800	1.38268600
H	-0.72420800	-1.96920400	-4.02510300
H	-0.60131600	1.01958400	-4.33406500
Br	-6.29216000	0.11277000	-0.49203300

Optimized Cartesian coordination of Lewis adduct of $B(C_6F_5)_3$ and 2

C	0.04075300	0.73392200	-3.11960300
H	-0.44666900	1.67839700	-2.95158100
H	-0.35841800	0.29298700	-4.03353200
C	0.11953300	-1.55700400	-2.58061800
H	1.13369100	-1.49782400	-2.95783400
H	0.05165800	-2.34933900	-1.84804800
C	-1.69553100	-0.14438500	-1.72089000
C	-2.22642500	1.07570900	-1.31223500
C	-2.54257600	-1.23242900	-1.86540200
C	-3.58017300	1.21102100	-1.06514100
H	-1.58611700	1.93369000	-1.16743200
C	-3.90481300	-1.10329200	-1.61645500
H	-2.17457200	-2.20555400	-2.14983600
C	-4.41865700	0.11690700	-1.22313200
H	-3.97772200	2.16468900	-0.74516700
H	-4.55416100	-1.96088300	-1.72972300
C	-0.41240200	-0.43469000	0.75936000
C	-0.94312100	0.48999800	1.65659600
C	-0.92798200	-1.71643500	0.93165800
C	-1.84789000	0.17274900	2.65728800
C	-1.83232300	-2.07911500	1.90787400
C	-2.29468000	-1.12412000	2.79261900
C	1.40267600	1.42261600	-0.04397500
C	2.28771500	1.41566700	1.03988500
C	1.26338200	2.68597800	-0.59912500
C	3.01299500	2.50676200	1.47834700
C	1.97113800	3.80847600	-0.19980700
C	2.86605900	3.72344700	0.84339700
C	1.99770200	-1.08149300	-0.49234500
C	2.32506800	-2.09829300	0.40377300
C	2.98857200	-0.85761800	-1.44292400
C	3.47780100	-2.86332000	0.31613900
C	4.15239200	-1.59117300	-1.56953500
C	4.39876000	-2.61894100	-0.68145000
N	-0.23855800	-0.22848300	-1.98923400
B	0.70761300	-0.05024500	-0.37683900
F	3.71391300	-3.82028000	1.20995300
F	1.56524700	-2.36988800	1.46859900
F	5.50511000	-3.34507500	-0.77710400
F	5.02827900	-1.31317400	-2.53401200
F	2.84265800	0.14151200	-2.33948200
F	2.44437600	0.30386200	1.77799800
F	0.35742500	2.93730900	-1.56600600
F	1.77095400	4.97464800	-0.81240700
F	3.55126400	4.78762900	1.24273500
F	3.83675900	2.39396400	2.51737500
F	-0.56714700	-2.70963900	0.09560900
F	-0.63249200	1.79451100	1.58596100
F	-2.30306400	1.12049000	3.47446800
F	-3.16865700	-1.44556500	3.73722200
F	-2.26835500	-3.33457900	1.99487300
H	-0.54239400	-1.76013100	-3.42120800
H	1.10831800	0.88071400	-3.21873600
Br	-6.27645800	0.29904800	-0.89074000

Optimized Cartesian coordination of *syn*-complex of $B(C_6F_5)_3$ and 5a

C	4.19185694	-1.89628550	-1.53265924
C	3.75135921	-2.00095994	-0.21162751
H	5.66316178	-2.53677730	-2.95348534
C	5.31934739	-2.61651109	-1.92728788
C	4.43894038	-2.82049516	0.68161893
C	5.55720198	-3.53388747	0.27917063
C	5.99987092	-3.43058467	-1.03527284
H	4.09298229	-2.89438259	1.70770473
H	6.08416779	-4.16341208	0.98633189
H	6.87295517	-3.98276155	-1.36244673
C	2.51008084	-1.25857453	0.24846406
H	1.65594219	-1.94354632	0.22853948
H	2.62563622	-0.95067698	1.28249281
C	2.10683614	-0.56705629	-1.99145750
H	1.42088854	-1.41733829	-2.00821972
H	1.65982318	0.20269394	-2.61693972
C	3.47181710	-1.00406832	-2.51998545
H	4.09194193	-0.12625746	-2.72549144
H	3.34870084	-1.52559737	-3.47266643
C	2.71895874	1.14185496	-0.31711423
C	2.99826538	1.53753402	1.00275490
C	2.93690357	2.09288067	-1.32706965
C	3.46063611	2.81199498	1.28774860
H	2.83275619	0.85961087	1.82674738
C	3.39666229	3.36790733	-1.02801465

H	2.74893928	1.84920990	-2.36227264
C	3.66570500	3.74550334	0.27890816
H	3.65791710	3.07674183	2.32045282
H	3.54760745	4.07114420	-1.83907774
H	4.02732727	4.74023433	0.50742330
C	-1.19235117	1.65606232	0.39396135
C	-1.37616089	2.39215793	1.56465647
C	-0.63368605	2.36403427	-0.67085546
C	-1.03855956	3.72485961	1.67791046
C	-0.27654009	3.69439064	-0.58872451
C	-0.47978384	4.37798657	0.59507040
C	-1.57149873	-0.80702018	1.50741484
C	-2.54756723	-1.78025704	1.70923034
C	-0.56602809	-0.76329426	2.46973372
C	-2.53837860	-2.64455854	2.78589067
C	-0.51340406	-1.62530071	3.54551350
C	-1.50990568	-2.57036895	3.70586267
C	-2.09399935	-0.41517024	-1.10717269
C	-2.98891217	0.27181560	-1.91970848
C	-1.67770461	-1.65276660	-1.58400161
C	-3.45239047	-0.23012384	-3.11890297
C	-2.10212858	-2.17628377	-2.78869319
C	-3.00108536	-1.46115522	-3.55759938
N	2.18294452	-0.12079106	-0.60282391
B	-1.60380130	0.15494204	0.27093505
F	-4.32395122	0.45732186	-3.85513352
F	-3.45868980	1.46673646	-1.54069480
F	-3.42854892	-1.95388169	-4.71262398
F	-1.65950567	-3.35879436	-3.21286104
F	-0.80609147	-2.38616235	-0.87814954
F	-3.57364139	-1.89662629	0.85867370
F	0.42112772	0.13249222	2.36900907
F	0.48054956	-1.55333155	4.42922680
F	-1.48014898	-3.39963097	4.73950406
F	-3.50628559	-3.54555954	2.94408874
F	-0.40911169	1.76102039	-1.84152201
F	-1.92477217	1.82396073	2.64354146
F	-1.24669239	4.38666137	2.81515629
F	-0.14950051	5.65775677	0.68974233
F	0.24542870	4.32652514	-1.63691033

Optimized Cartesian coordination of *anti*-complex of $B(C_6F_5)_3$ and 5a

C	-4.98304000	-1.60005000	0.06208900
H	-4.16659400	-2.10892100	-0.45999900
H	-5.58237300	-2.37467900	0.56743400
N	-4.41062500	-0.65953000	1.02180800
C	-5.07068600	0.62258500	1.27174700
H	-5.01033600	0.84787100	2.34400500
H	-4.52734300	1.43367000	0.75473700
C	-3.17383500	-0.90641300	1.60178500
C	-2.59362400	-2.19769100	1.57589200
H	-3.13444900	-3.02860800	1.13724000
C	-1.34459000	-2.43367500	2.14336700
H	-0.93046000	-3.43804100	2.10245600
C	-0.62874400	-1.40973600	2.76721100
C	-1.19687300	-0.13659100	2.81441800
H	-0.66372900	0.68041900	3.29496200
C	-2.44222100	0.12054000	2.24404200
H	-2.83102300	1.13097700	2.27820800
B	2.20804900	0.14293900	-0.47961200
C	0.82242800	-0.23570800	-1.10734600
C	0.65627100	-1.33704000	-1.96299300
C	-0.56733500	-1.69343900	-2.51682700
C	-1.69496000	-0.93499100	-2.21281200
C	-1.58467200	0.17155400	-1.37718600
C	-0.34468700	0.50091800	-0.84368200
F	1.71170500	-2.09371400	-2.30601800
F	-0.67274200	-2.74967300	-3.33014300
F	-2.88543900	-1.27787900	-2.71270600
F	-2.67178400	0.89921500	-1.09159700
F	-0.30919400	1.56112700	-0.02345800
C	2.57188000	1.65180000	-0.23509500
C	2.23874900	2.66186100	-1.14925500
C	2.56528300	3.99922000	-0.95619800
C	3.23810600	4.37481400	0.20468600
C	3.58280800	3.41047500	1.14927300
C	3.25719500	2.07999300	0.91131100
F	1.59828400	2.35458600	-2.28995100
F	2.24094900	4.92283000	-1.86701400
F	3.55093900	5.65337100	0.41089600
F	4.22103300	3.77077000	2.26756800
F	3.60629900	1.19383400	1.85924800
C	3.24538900	-0.97113200	-0.09443300
C	4.62941900	-0.78633300	-0.24415800
C	5.56787900	-1.75599500	0.08996000
C	5.13441500	-2.96978600	0.61843800
C	3.77204800	-3.20065200	0.79594800
C	2.86171200	-2.21529600	0.43138300
F	5.10862800	0.35814400	-0.75950600
F	6.87433300	-1.53567900	-0.08910100
F	6.02013400	-3.90682000	0.95220800
F	3.35434400	-4.36241800	1.30944000
F	1.56433900	-2.49409300	0.63270900
H	0.34304700	-1.60357900	3.21074200
C	-6.52062500	0.65446400	0.84343900
C	-7.46030800	1.42001200	1.53920600
C	-6.91247200	-0.05766500	-0.29860400
C	-8.78226400	1.48943700	1.09810700
H	-7.15651100	1.96321000	2.43160500
C	-8.24074000	0.00389400	-0.72805300
C	-9.17359500	0.77957000	-0.03855000
H	-9.50583100	2.08701900	1.64594200
H	-8.54490000	-0.55983800	-1.60734900
H	-10.20382000	0.82223800	-0.38178800

C	-5.85377500	-0.88445700	-0.97924000
H	-6.30263500	-1.62880300	-1.64658300
H	-5.20256100	-0.25028100	-1.59663900

Optimized Cartesian coordination of Lewis adduct of $B(C_6F_5)_3$ and 5a

C	3.91247114	-2.03808946	-0.85919905
C	3.31632008	-2.19214542	0.38524505
H	5.69363424	-2.33705063	-2.01604114
C	5.22536521	-2.46594760	-1.04606006
C	4.03138709	-2.77322353	1.43089913
C	5.33209114	-3.20921567	1.23653811
C	5.93181121	-3.05408971	-0.00924198
H	3.56353904	-2.88345050	2.40317120
H	5.88015515	-3.66118375	2.05426618
H	6.95038327	-3.38706582	-0.16856700
C	1.87994401	-1.79720727	0.60746006
H	1.22830189	-2.60565627	0.30335604
H	1.70760101	-1.62561924	1.65389514
C	1.70200106	-1.02311020	-1.62626011
H	1.07830594	-1.90183121	-1.75452212
H	1.32782609	-0.27097811	-2.30449916
C	3.14809114	-1.37947835	-1.97333614
H	3.70114425	-0.50263732	-2.31086516
H	3.09804608	-2.04922239	-2.83593820
C	2.32314024	0.57150087	0.19546103
C	2.56213428	0.82930287	1.53990413
C	2.86302235	1.42216389	-0.76154004
C	3.34228943	1.91320589	1.91737617
H	2.14187319	0.20693886	2.31276619
C	3.64290950	2.50442591	-0.37882601
H	2.67830933	1.27396390	-1.81371212
C	3.89124454	2.75456891	0.96201909
H	3.51568046	2.09477389	2.97082524
H	4.05301059	3.15343192	-1.14254007
H	4.50172166	3.59823192	1.25877212
C	-0.20398087	1.56001416	-0.46793102
C	-0.27220779	2.55129424	0.51198106
C	-0.03218481	2.08525519	-1.74712812
C	-0.24749068	3.91127935	0.25449304
C	-0.00594970	3.43245829	-2.04944214
C	-0.12374263	4.36336837	-1.03985706
C	-1.12003309	-0.20074790	1.36669612
C	-2.45613816	0.20781025	1.28140912
C	-0.79848510	-0.65604896	2.63760122
C	-3.37856423	0.14337932	2.30599819
C	-1.69007518	-0.74273989	3.69566730
C	-2.99695824	-0.34624575	3.53660529
C	-1.19515316	-1.01555695	-1.08829907
C	-2.01348619	-0.60174785	-2.13984015
C	-1.35472629	-2.36945504	-0.79410904
C	-2.80220832	-1.45646585	-2.89294721
C	-2.12810842	-3.25723005	-1.51643610
C	-2.85290244	-2.79994795	-2.59549618
N	1.45791808	-0.57938414	-0.19124700
B	-0.28679001	-0.04857295	-0.08144399
F	-3.54443434	-0.97317975	-3.89268528
F	-2.16185809	0.68955426	-2.46187517
F	-3.60924057	-3.62885795	-3.30939823
F	-2.19237654	-4.54286614	-1.16323207
F	-0.75781829	-2.90317813	0.29000804
F	-2.92807915	0.74384333	0.14031203
F	0.45146096	-1.03186009	2.97376325
F	-1.27577518	-1.20347496	4.87901239
F	-3.86450132	-0.42168868	4.54309937
F	-4.63215229	0.56035846	2.11338718
F	0.18100314	1.28278411	-2.80814120
F	-0.34170782	2.24501623	1.81822716
F	-0.32965361	4.78745242	1.25879411
F	-0.09367552	5.66581349	-1.30751008
F	0.15636735	3.83782831	-3.31163324

VII. Borane-catalyzed carbon–carbon bond-forming reaction under dark condition and photoirradiation

Substrate preparation

N-methyl-*N*-(TMSCH$_2$)anilines (**1a** and **1b**)[15] and *N*-aryltetrahydroisoquinolines (**5a**, **5b**, **5c**, and **5d**)[16] were prepared by following the literature procedures. Methyl vinyl ketone (**3a**) and ethyl vinyl ketone (**3b**) were purchased and distilled prior to use. (*E*)-1-Phenylbut-2-ene-1-one (**3c**) was synthesized by following the literature procedure[17] and purified by column chromatography on silica gel.

General procedure for borane-catalyzed coupling reactions of *N*-alkylaniline derivatives with α,β-unsaturated ketones

To a 10 mL reaction tube equipped with a magnetic stir bar, aniline derivative **1**, **2**, or **5** (0.100 mmol), and B(C_6F_5)$_3$ (10.0 μmol, 10 mol% for the aniline) were added. The tube was capped with a rubber septum and degassed *in vacuo* and backfilled with argon three times (and the test tube was wrapped with aluminum foil for **1**). Then, 1.0 mL of solvent (CH_2Cl_2, Et_2O, THF, DCE, or MeCN (and 0.1 mL of MeOH, if necessary)) was introduced via a syringe and α,β-unsaturated ketone **3** was added. The mixture was stirred at room temperature under 405 nm LED irradiation (for **2** and **5**). Volatiles were removed *in vacuo* and the residues were purified by silica gel column chromatography to afford the coupling product, if otherwise noted. The yield of **6f** was reported as a mixture of diastereomers after the purification by silica gel column chromatography and the diastereomer ratio was determined by ^{1}H NMR analysis. The diastereomers were separated by further purification with a recycle HPLC.

Effect of solvent, light source, and catalyst on the profile of the reaction of **5a** with **3a**

Table S5 Light source and catalyst screening

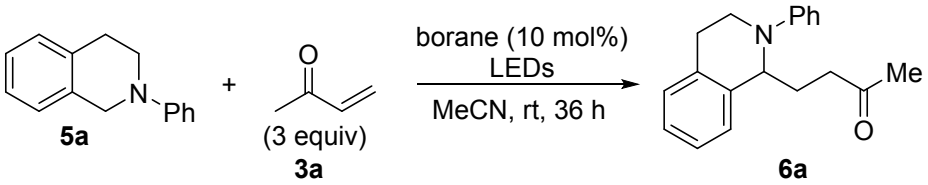

entry	LED (peak top, nm)	borane	yield(%) of **6a**
1[a]	405	B(C_6F_5)$_3$	31
2	405	B(C_6F_5)$_3$	70
3	448	B(C_6F_5)$_3$	9
4	–	B(C_6F_5)$_3$	no reaction
5	405	BPh_3	9
6	405	BF_3•OEt_2	0

[a]in DCE

[15] L. R. Espelt, I. S. McPherson, E. M. Wiensch, T. P. Yoon, *J. Am. Chem. Soc.*, 2015, **137**, 2452.
[16] (a) F. Y. Kwong, A. Klapars, S. L. Buchwald, *Org. Lett.*, 2002, **4**, 581. (b) D. P. Hari, B. König, *Org. Lett.*, 2011, **13**, 3852. (c) A. M. Nauth, N. Otto, T. Opatz, *Adv. Synth. Catal.,* 2015, **357**, 3424. (d) L. R. Espelt, E. M. Wiensch, T. P. Yoon, *J. Org. Chem.,* 2013, **78**, 4107.
[17] K. Kumar, S. S. More, S. Goyal, M. Gangar, G. L. Khatik, R. K. Rawal, V. A. Nair, *Tetrahedron Lett.*, 2016, **57**, 2315.

Light on/off experiment in the reaction of **5a** with **3a** under the influence of $B(C_6F_5)_3$

The reactions were performed according to the general procedure in five independent test tubes, which were corresponding to each plot, respectively. After the removal of the volatiles *in vacuo*, 1,3,5-trimethoxybenzene was added to the crude mixture as an internal standard for the calculation of NMR yield of **6a**. The NMR spectra were recorded in $CDCl_3$.

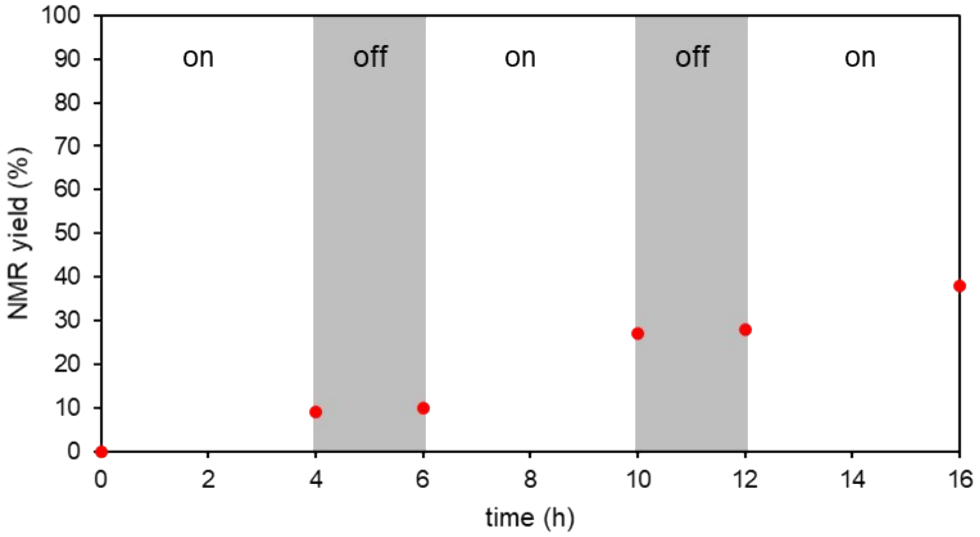

Fig. S14 Time profile of the reaction of **5a** with **3a** catalyzed by $B(C_6F_5)_3$.

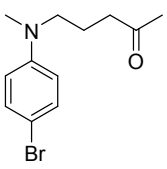

5-((4-bromophenyl)(methyl)amino)pentane-2-one (4a)

^{1}H NMR (400 MHz, $CDCl_3$): δ 7.28 (d, *J* = 9.2 Hz, 2H), 6.57 (d, *J* = 9.2 Hz, 2H), 3.29 (t, *J* = 7.2 Hz, 2H), 2.88 (s, 3H), 2.45 (t, *J* = 7.2 Hz, 2H), 2.12 (s, 3H), 1.84 (tt, *J* = 7.2, 7.2 Hz, 2H); ^{13}C NMR (151 MHz, $CDCl_3$): δ 208.3, 148.4, 132.0, 113.9, 108.2, 51.9, 40.6, 38.4, 30.2, 20.9; IR (film): 2931, 1715, 1590, 1500, 1368, 1212, 1191, 1167, 1119, 1079, 809 cm^{-1}; HRMS-ESI (*m*/*z*): $[M+H]^+$ Calcd for $C_{12}H_{17}BrNO^+$, 270.0488; Found, 270.0479.

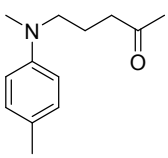

5-(methyl(*p*-tolyl)amino)pentane-2-one (4b)

^{1}H NMR (500 MHz, $CDCl_3$): δ 7.03 (d, *J* = 8.8 Hz, 2H), 6.64 (d, *J* = 8.8 Hz, 2H), 3.27 (t, *J* = 7.1 Hz, 2H), 2.87 (s, 3H), 2.46 (t, *J* = 7.1 Hz, 2H), 2.24 (s, 3H), 2.11(s, 3H), 1.85 (tt, *J* = 7.1, 7.1 Hz, 2H); ^{13}C NMR (151 MHz, $CDCl_3$): δ 208.6, 147.6, 129.9, 125.8, 112.9, 52.3, 40.9, 38.5, 30.1, 21.1, 20.3; IR (film): 2921, 2860, 1684, 1617, 1519, 1449, 1360, 1219, 1202, 1180, 1116, 975, 803, 753 cm^{-1}; HRMS-ESI (*m*/*z*): $[M+H]^+$ Calcd for $C_{13}H_{20}ON^+$, 206.1539; Found, 206.1542.

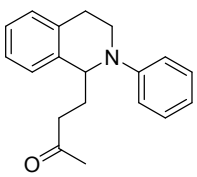

4-(2-phenyl-1,2,3,4-tetrahydroisoquinolin-1-yl)butan-2-one (6a)

^{1}H NMR (400 MHz, $CDCl_3$): δ 7.24-7.19 (m, 2H), 7.17-7.11 (m, 3H), 7.11-7.07 (m, 1H), 6.88 (d, *J* = 8.4 Hz, 2H), 6.73 (t, *J* = 7.4 Hz, 1H), 4.72 (dd, *J* = 9.2, 5.6 Hz, 1H), 3.61 (ddd, *J* = 13.2, 6.0, 4.6 Hz, 1H), 3.55 (ddd, *J* = 13.2, 9.8, 4.6 Hz, 1H), 2.99 (ddd, *J* = 16.3, 9.8, 6.0 Hz, 1H), 2.74 (ddd, *J* = 16.3, 4.6, 4.6 Hz, 1H), 2.56 (t, *J* = 6.8 Hz, 2H), 2.22 (ddt, *J* = 14.4, 9.2, 6.8 Hz 1H), 2.09 (s, 3H), 2.05 (dtd, *J* = 14.4, 6.8, 5.6 Hz, 1H); ^{13}C NMR (151 MHz, $CDCl_3$): δ 208.7, 150.0, 138.5, 135.0, 129.5, 128.9, 127.4, 126.7, 126.1, 117.9, 114.7, 58.1, 41.6, 40.5, 30.5, 30.4, 26.5; IR (film): 3022, 2924, 1710, 1597, 1503, 1492, 1394, 1363, 1351, 1324, 1220, 1159, 748 cm^{-1} ; HRMS-ESI (*m*/*z*): $[M+H]^+$ Calcd for $C_{19}H_{22}NO^+$, 280.1696; Found, 280.1693.

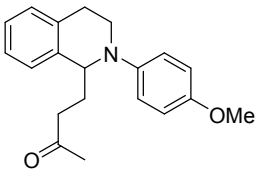

4-(2-(4-methoxyphenyl)-1,2,3,4-tetrahydroisoquinolin-1-yl)butan-2-one (6b)

^{1}H NMR (400 MHz, $CDCl_3$): δ 7.18-7.10 (m, 3H), 7.06 (d, *J* = 6.8 Hz, 1H), 6.87-6.82 (m, 2H), 6.81-6.76 (m, 2H), 4.51 (dd, *J* = 9.6, 5.2 Hz, 1H), 3.74 (s, 3H), 3.49 (dd, *J* = 8.2, 4.2 Hz, 2H), 2.89 (dt, *J* = 16.5, 8.2 Hz, 1H), 2.64 (dt, *J* = 16.5, 4.2 Hz, 1H), 2.56 (t, *J* = 7.0 Hz, 2H), 2.18 (ddt, *J* = 14.4, 9.6, 7.0 Hz, 1H), 2.09 (s, 3H), 2.03 (dtd, *J* = 14.4, 7.0, 5.2 Hz, 1H); ^{13}C NMR (151 MHz, $CDCl_3$): δ 208.9, 153.1, 144.7, 138.6, 135.0, 129.0, 127.4, 126.5, 126.1, 118.4, 114.8, 58.9, 55.8, 43.2, 40.6, 30.8, 30.5, 26.0; IR (film): 2935, 2832, 1709, 1507, 1361, 1240, 1181, 1159, 1035, 948, 818, 752 cm^{-1}; HRMS-ESI (*m*/*z*): $[M+H]^+$ Calcd for $C_{20}H_{24}NO_2^+$, 310.1802; Found, 310.1790.

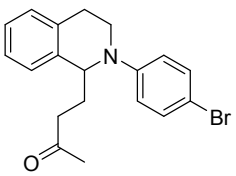

4-(2-(4-bromophenyl)-1,2,3,4-tetrahydroisoquinolin-1-yl)butan-2-one (6c)

^{1}H NMR (400 MHz, $CDCl_3$): δ 7.31-7.26 (m, 2H), 7.20-7.08 (m, 4H), 6.78-6.73 (m, 2H), 4.67 (dd, *J* = 8.8, 6.0 Hz, 1H), 3.53 (dd, *J* = 7.4, 5.0 Hz, 2H), 2.96 (dt, *J* = 16.4, 7.4 Hz, 1H), 2.78 (dt, *J* = 16.4, 5.0 Hz, 1H), 2.53 (t, *J* = 6.8 Hz, 2H), 2.20 (ddt, *J* = 14.0, 8.8, 6.8 Hz, 1H), 2.09 (s, 3H), 2.01 (dtd, *J* = 14.0, 6.8, 6.0 Hz, 1H); ^{13}C NMR (151 MHz, $CDCl_3$): δ 208.5, 148.9, 138.0, 134.8, 132.1, 128.9, 127.4, 126.9, 126.2, 116.1, 109.6, 58.0, 41.9, 40.3, 30.4, 30.3, 26.5; IR (film) 2923, 1711, 1587, 1492, 1395, 1337, 1221, 1159, 948, 805, 759 cm^{-1}; HRMS-ESI (*m*/*z*): $[M+H]^+$ Calcd for $C_{19}H_{21}NOBr^+$, 358.0801; Found, 358.0789.

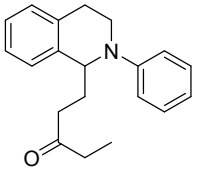

5-(2-phenyl-1,2,3,4-tetrahydroisoquinolin-1-yl)pentan-3-one (6e)

^{1}H NMR (400 MHz, $CDCl_3$): δ 7.22 (dd, *J* = 8.0, 7.4 Hz, 2H), 7.18-7.11 (m, 3H), 7.11-7.06 (m, 1H), 6.87 (d, *J* = 8.0 Hz, 2H), 6.73 (t, *J* = 7.4, 1H), 4.73 (dd, *J* = 9.0, 5.4 Hz, 1H), 3.61 (ddd, *J* = 14.0, 6.0, 4.6 Hz, 1H), 3.55 (ddd, *J* = 14.0, 9.6, 4.6 Hz 1H), 2.99 (ddd, *J* = 16.1, 9.6, 6.0 Hz, 1H), 2.74 (ddd, *J* = 16.1, 4.6, 4.6 Hz, 1H), 2.54 (t, *J* = 7.0 Hz, 2H), 2.36 (q, *J* = 7.4 Hz, 2H), 2.24 (ddt, *J* = 14.4, 9.0, 7.0 Hz, 1H), 2.06 (dtd, *J* = 14.4, 7.0, 5.4 Hz, 1H), 1.02 (t, *J* = 7.4 Hz, 3H); ^{13}C NMR (151 MHz, $CDCl_3$): δ 211.4, 150.0, 138.6, 135.0, 129.4, 128.9, 127.4, 126.7, 126.1, 117.8, 114.7, 58.1, 41.6, 39.2, 36.3, 30.6, 26.5, 8.0; IR (film): 2935, 1709, 1596, 1503, 1492, 1393, 1323, 1219, 986, 908, 746 cm^{-1}; HRMS-ESI (*m*/*z*): $[M+H]^+$ Calcd for $C_{20}H_{24}NO^+$, 294.1852; Found, 294.1864.

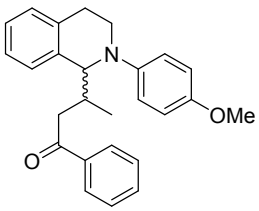

3-(2-(4-methoxyphenyl)-1,2,3,4-tetrahydroisoquinolin-1-yl)-1-phenyl-butan-1-one (6f)

major diastereomer; ^{1}H NMR (400 MHz, $CDCl_3$): δ 7.85-7.81 (m, 2H), 7.48 (tt, *J* = 7.2, 1.5 Hz, 1H), 7.36 (dd, *J* = 7.6, 7.2 Hz, 2H), 7.19-7.13 (m, 3H), 7.12-7.07 (m, 1H), 6.71-6.67 (m, 2H), 6.67-6.62 (m, 2H), 4.25 (d, *J* = 9.6 Hz, 1H), 3.71 (s, 3H), 3.58 (dt, *J* = 12.9, 6.7 Hz, 1H), 3.43 (dd, *J* = 15.5, 5.6 Hz, 1H), 3.25 (dt, *J* = 12.9, 6.3 Hz, 1H), 2.85 (dd, *J* = 6.7, 6.3 Hz, 2H), 2.77 (ddqd, *J* = 9.6, 7.4, 6.4, 5.6 Hz, 1H), 2.68 (dd, *J* = 15.5, 7.4 Hz, 1H), 1.08 (d, *J* = 6.4 Hz, 3H); ^{13}C NMR (151 MHz, $CDCl_3$): δ 199.5, 152.5, 144.7, 137.6, 137.0, 135.7, 132.6, 128.9, 128.8, 128.5, 128.2, 126.9, 125.4, 117.0, 114.6, 64.3, 55.8, 44.5, 43.6, 37.1, 26.4, 18.9; IR (film): 2930, 2832, 1678, 1507, 1491, 1463, 1269, 1243, 1038, 1002, 816, 750 cm^{-1};

minor diastereomer; ^{1}H NMR (600 MHz, $CDCl_3$): δ 7.76 (d, *J* = 7.2 Hz, 2H), 7.50 (t, *J* = 7.8 Hz, 1H), 7.38 (dd, *J* = 7.8, 7.2 Hz, 2H), 7.22 (dd, *J* = 7.8, 1.8 Hz, 1H), 7.19-7.12 (m, 3H), 6.87 (d, *J* = 9.0 Hz, 2H), 6.76 (d, *J* = 9.0 Hz, 2H), 4.59 (d, *J* = 6.6 Hz, 1H), 3.72 (s, 3H), 3.70 (ddd, *J* = 12.5, 6.6, 6.6 Hz, 1H), 3.45 (ddd, *J* = 12.5, 6.3, 6.3 Hz, 1H), 3.23 (dd, *J* = 15.2, 3.3 Hz, 1H), 2.93 (ddd, *J* = 16.5, 6.6, 6.3 Hz, 1H), 2.89 (ddd, *J* = 16.5, 6.6, 6.3 Hz, 1H), 2.78-2.72 (m, 1H), 2.72 (dd, *J* = 15.2, 8.4 Hz, 1H), 1.06 (d, *J* = 6.0 Hz, 3H); ^{13}C NMR (151 MHz, $CDCl_3$): δ 200.3, 152.6, 145.6, 137.4, 136.0, 132.9, 128.8, 128.6, 128.14, 128.08, 126.7, 125.8, 117.8, 114.7, 63.2, 55.8, 45.5, 43.0, 36.8, 27.2,17.6, one peak for aromatic carbon was not found probably due to overlapping; IR (film): 2928, 2832, 1679, 1597, 1507, 1448, 1268, 1243, 1218, 1037, 751 cm^{-1}; HRMS-ESI (*m*/*z*): $[M+H]^+$ Calcd for $C_{26}H_{28}NO_2^+$, 386.2115; Found, 386.2104.

^{1}H NMR monitoring for the formation of **4b** from **1b** and **3a** catalyzed by $B(C_6F_5)_3$

Under nitrogen atmosphere, $B(C_6F_5)_3$ (3.84 mg, 0.075 mmol, 10 mol%) was added to a screw-capped NMR tube wrapped in aluminum foil. Subsequently, THF-d_8 (0.75 mL), **1b** (15.5 mg, 0.75 mmol), and freshly distilled **3a** (29.7 μL, 0.375 mmmol, 5 equiv) were added to the tube with syringes and the tube was shaken. Except for the NMR measurement, the sample tube was stored under dark condition by wrapping with aluminum foil. Through the monitoring time, no signal assignable to silyl enol ether was observed.

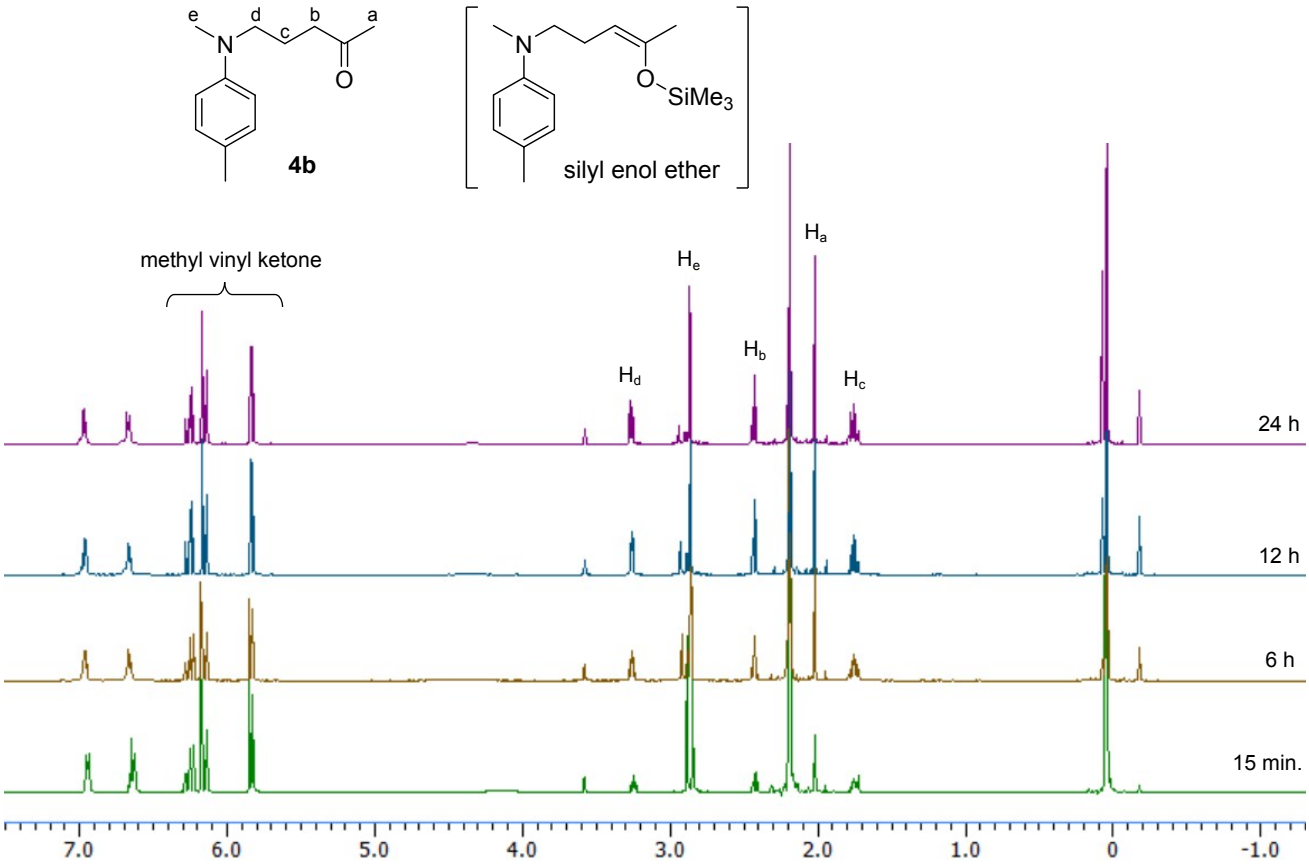

Fig. S15 ^{1}H NMR monitoring of the reaction of **1b** and **3a** catalyzed by $B(C_6F_5)_3$ in THF-d_8.

Deuterium incorporation experiment in Scheme 1

The experiment was conducted by the general procedure described in section VII except for using MeOD instead of MeOH. The incorporated deuterium ratio was calculated by the relative integral value of internal α-proton at 2.46 ppm in Fig. S16. In addition, no H-D exchange of isolated **4b** was observed in the condition of deuterium incorporation experiment (Scheme S1).

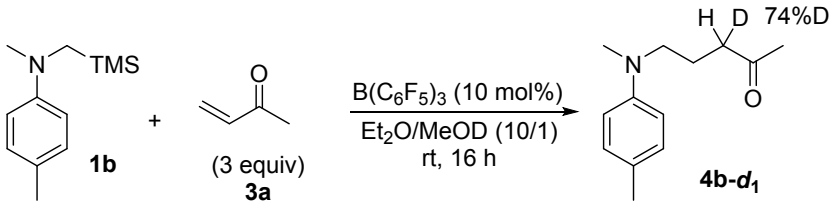

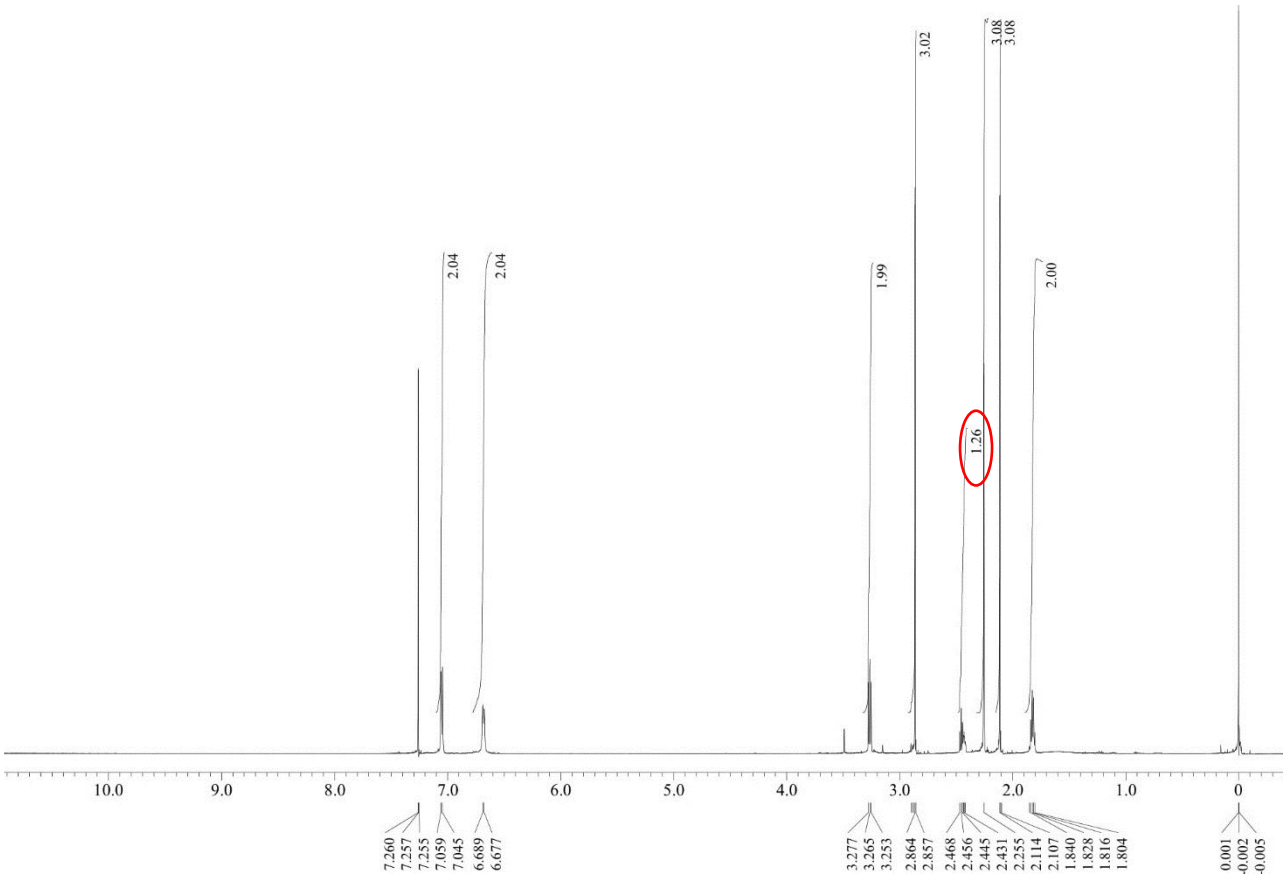

Fig. S16 ^{1}H NMR spectrum of crude **4b-*d*$_1$** (400 MHz, $CDCl_3$).

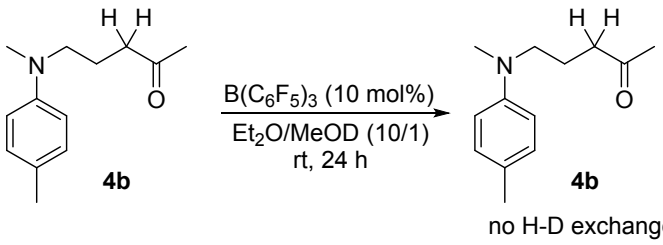

Scheme S1 H-D exchange experiment of isolated **4b** in the presence of $B(C_6F_5)_3$ and MeOD.

Crossover experiments under dark conditions

Crossover experiments were conducted by stirring a mixture of **1b** (0.10 mmol), **2** or **5a** (1.0 mmol), **3a** (1.0 mmol), and $B(C_6F_5)_3$ (0.010 mmol) in Et_2O (1.0 mL) and MeOH (0.1 mL) at room temperature for 16 h under dark conditions, in which only **1b** could be oxidized by $B(C_6F_5)_3$. If **4a** or **6a** were obtained, it would indicate the intervention of a radical-chain process as hydrogen-atom abstraction from **2** or **5a** by the initially generated, **1b**-derived α-aminomethyl radical or the transiently formed α-keto radical could generate the corresponding α-aminomethyl radical. However, **4a** and **6a** were not detected in the crude mixture by the ^1H NMR and ESI-MS analyses, and only **4b** was obtained as a sole product (Scheme S2, eqs. 1 and 2). The crossover reaction of eq. 1 was also conducted in DCE instead of Et_2O/MeOH, which gave **4b** in 41% isolated yield and the formation of **4a** was not observed.

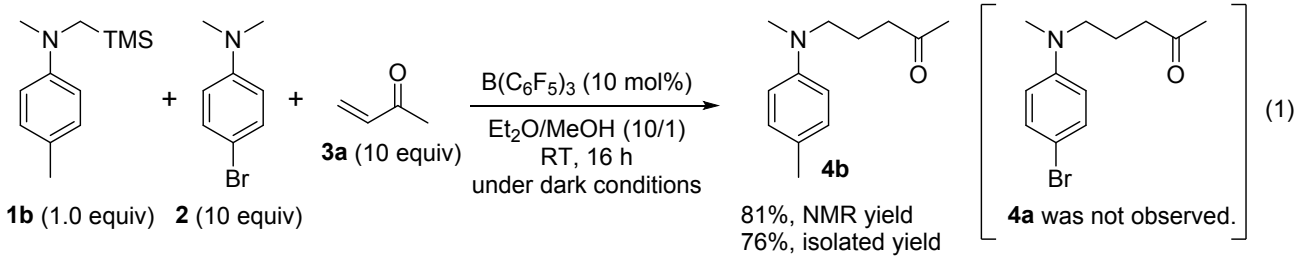

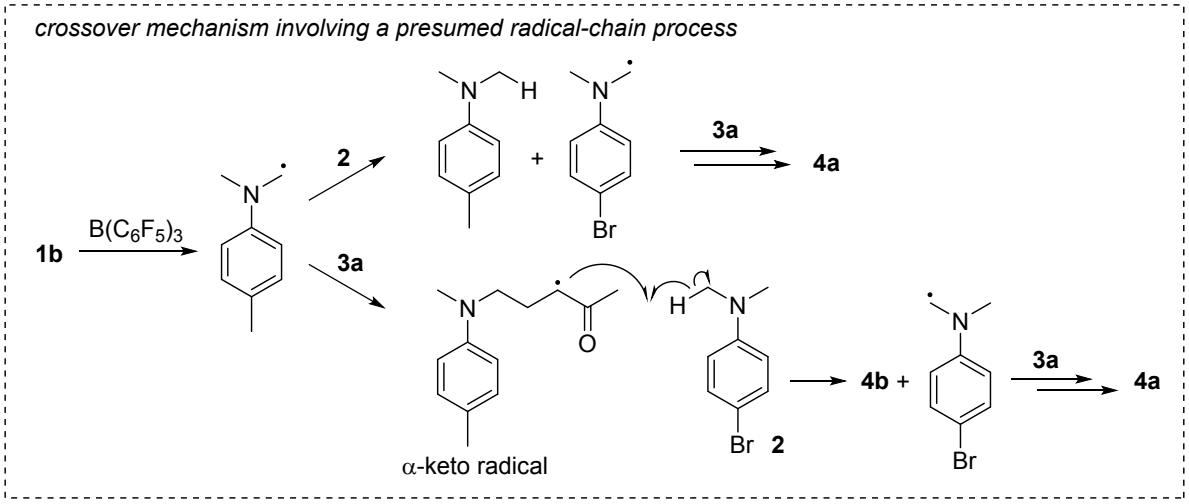

Scheme S2 Crossover experiments with **1b** and excess amount of **2** or **5a** and **3a** in the presence of a catalytic amount of $B(C_6F_5)_3$ under dark conditions. A possible crossover mechanism is shown in the hashed square.

VIII. NMR spectra

Lewis adduct of $B(C_6F_5)_3$ and **2**was not observed both in ^1H and ^{11}B NMR spectra in CD_2Cl_2 even at −90 °C, which showed only free $B(C_6F_5)_3$ and **2**, respectively.

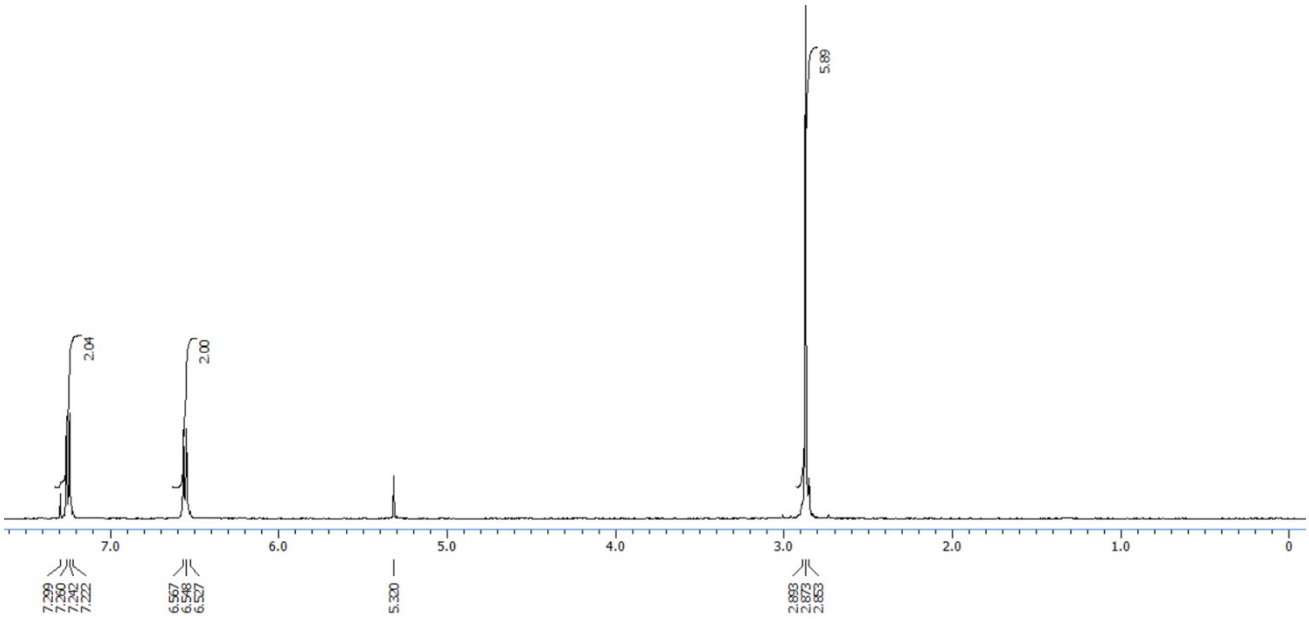

Fig. S17 ^1H NMR spectrum of a mixture of $B(C_6F_5)_3$ and **2** (0.1 M) at −90 °C (500 MHz, CD_2Cl_2).

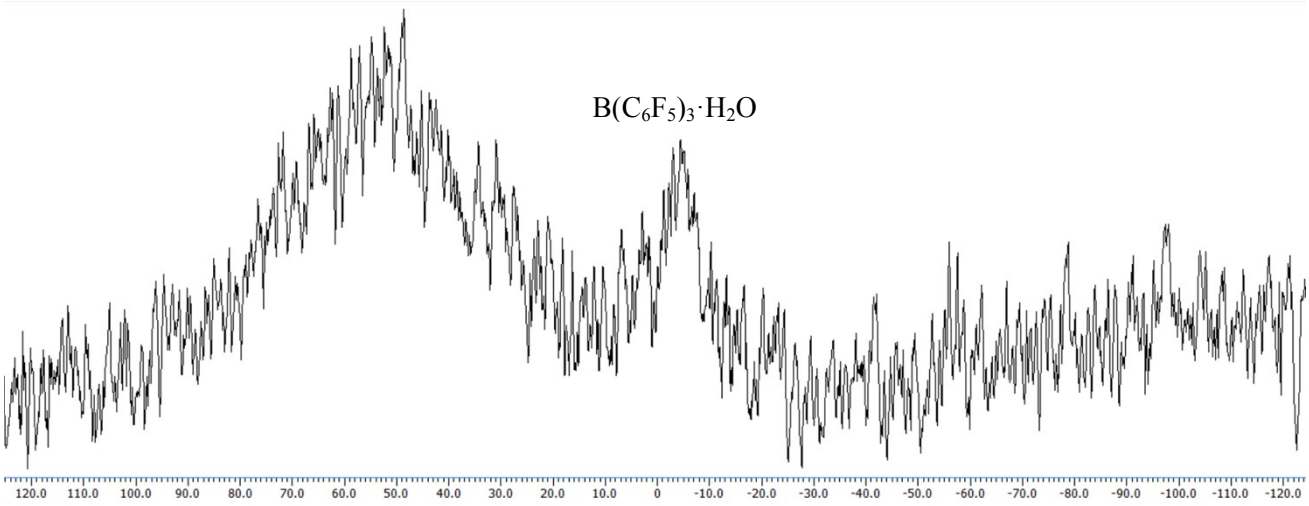

Fig. S18 ^{11}B NMR spectrum of a mixture of $B(C_6F_5)_3$ and **2** (0.1 M) at −90 °C (161 MHz, CD_2Cl_2).

NMR spectra under the reaction conditions reported in Table 2

Under the reaction conditions of Table 2, chemical shifts of the signals corresponding to **3a** and **5a** did not change in ^{1}H NMR (Fig. S19), indicating no Lewis adduct formation between $B(C_6F_5)_3$ and either **3a** or **5a**. In addition, only a Lewis adduct between $B(C_6F_5)_3$ and CD_3CN was detected in ^{11}B NMR (Fig. S20). These observations suggested that almost all $B(C_6F_5)_3$ formed a Lewis adduct with MeCN under the reaction conditions of Table 2, and the concentration of free $B(C_6F_5)_3$ and other Lewis adducts was very low.

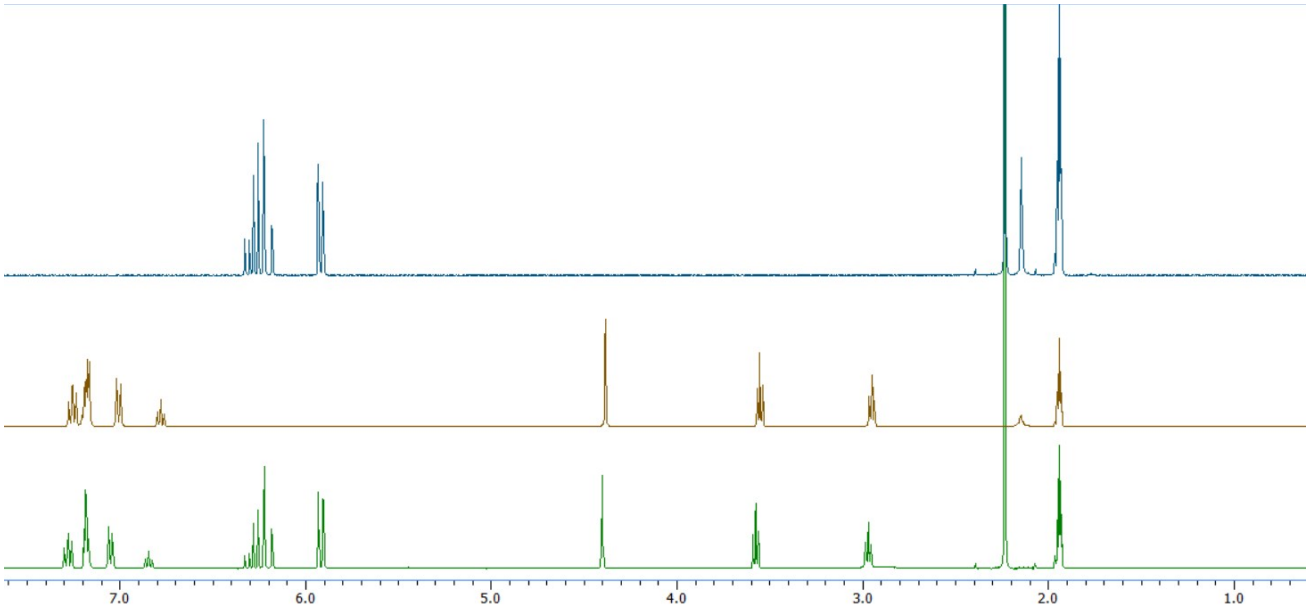

Fig. S19 ^{1}H NMR spectra of methyl vinyl ketone **3a** (blue), **5a** (brown), and the reaction mixture (green) in the concentration reported in Table 2 (**3a**: 0.3 M, **5a**: 0.1 M, and $B(C_6F_5)_3$: 0.01 M) (400 MHz, CD_3CN).

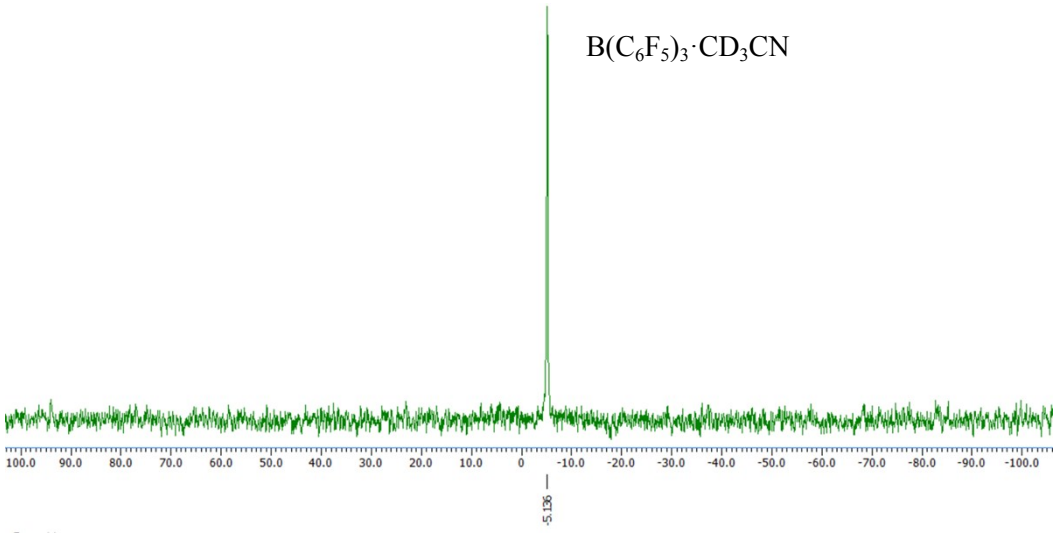

Fig. S20 ^{11}B NMR spectrum of the reaction mixture in the concentration reported in Table 2 (128 MHz, CD_3CN).

Copies of ^{1}H and ^{13}C NMR spectra:

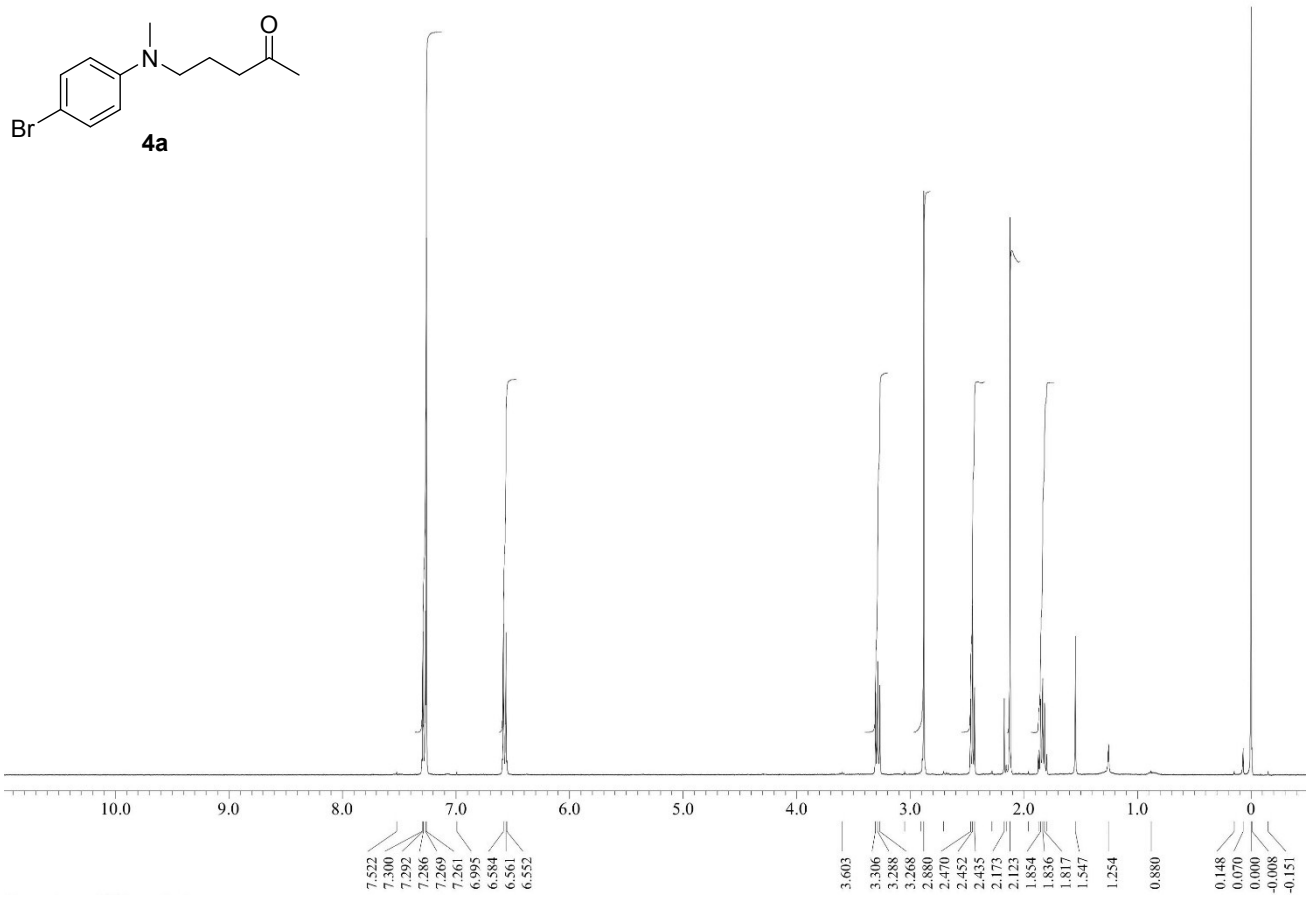

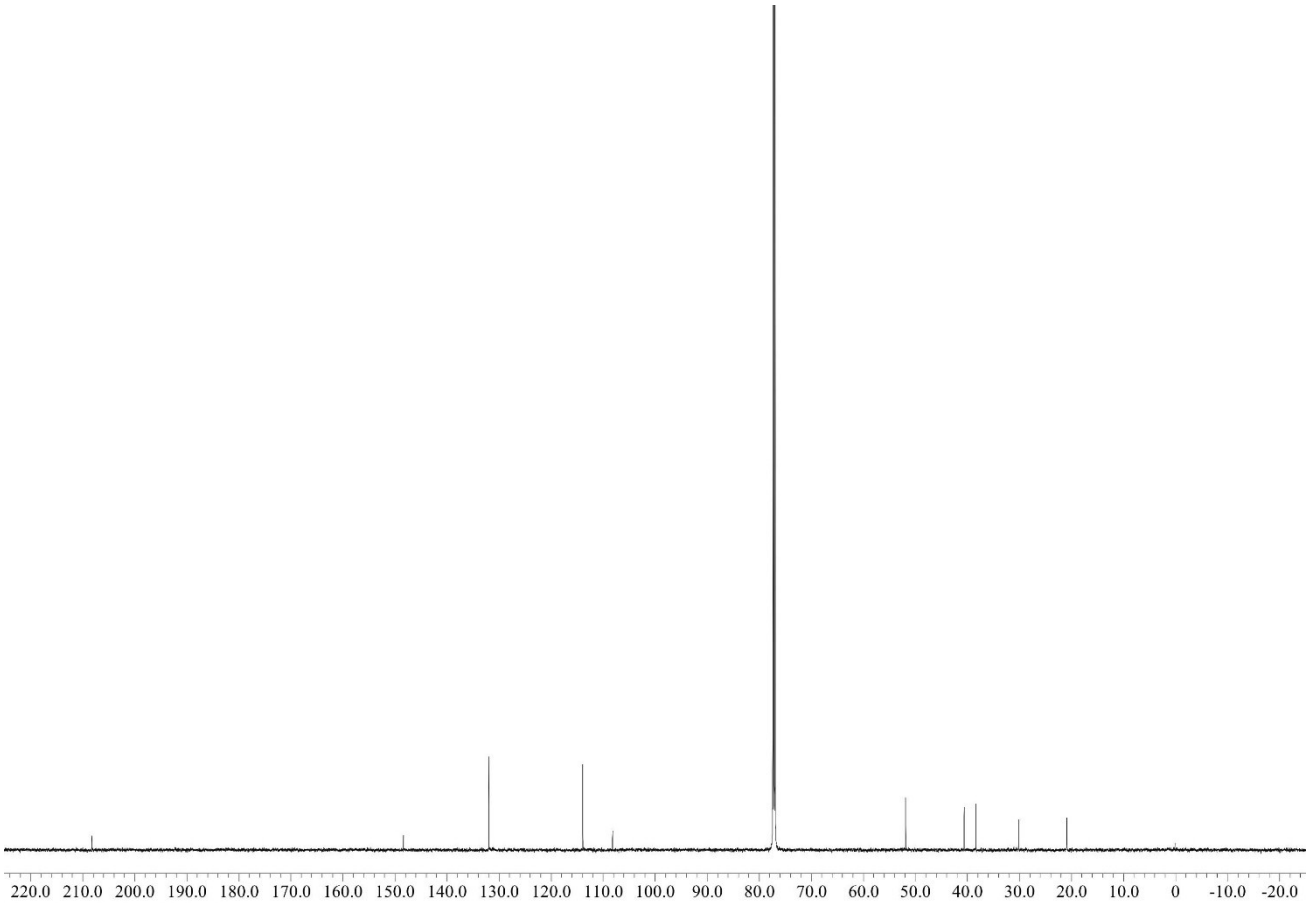

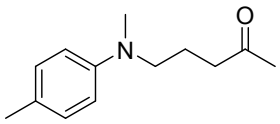

4b

10.0
9.0
8.0
7.0
6.0
5.0
4.0
3.0
2.0
1.0
0

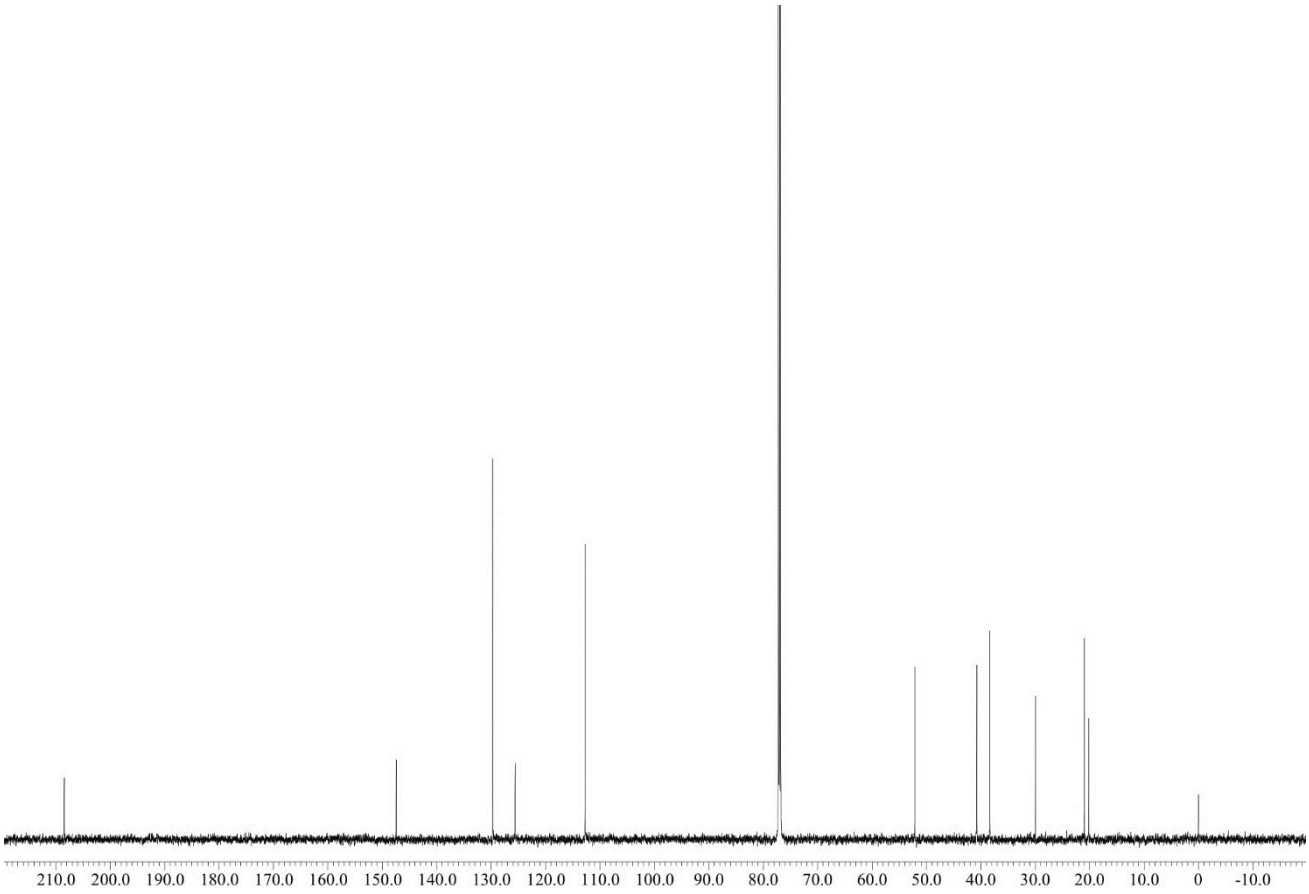
210.0
200.0
190.0
180.0
170.0
160.0
150.0
140.0
130.0
120.0
110.0
100.0
90.0
80.0
70.0
60.0
50.0
40.0
30.0
20.0
10.0
0
-10.0

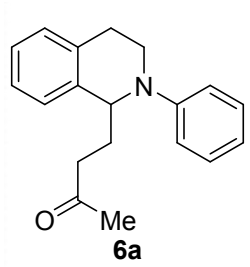
N
O
Me

6a

11.0
10.0
9.0
8.0
7.0
6.0
5.0
4.0
3.0
2.0
1.0
0

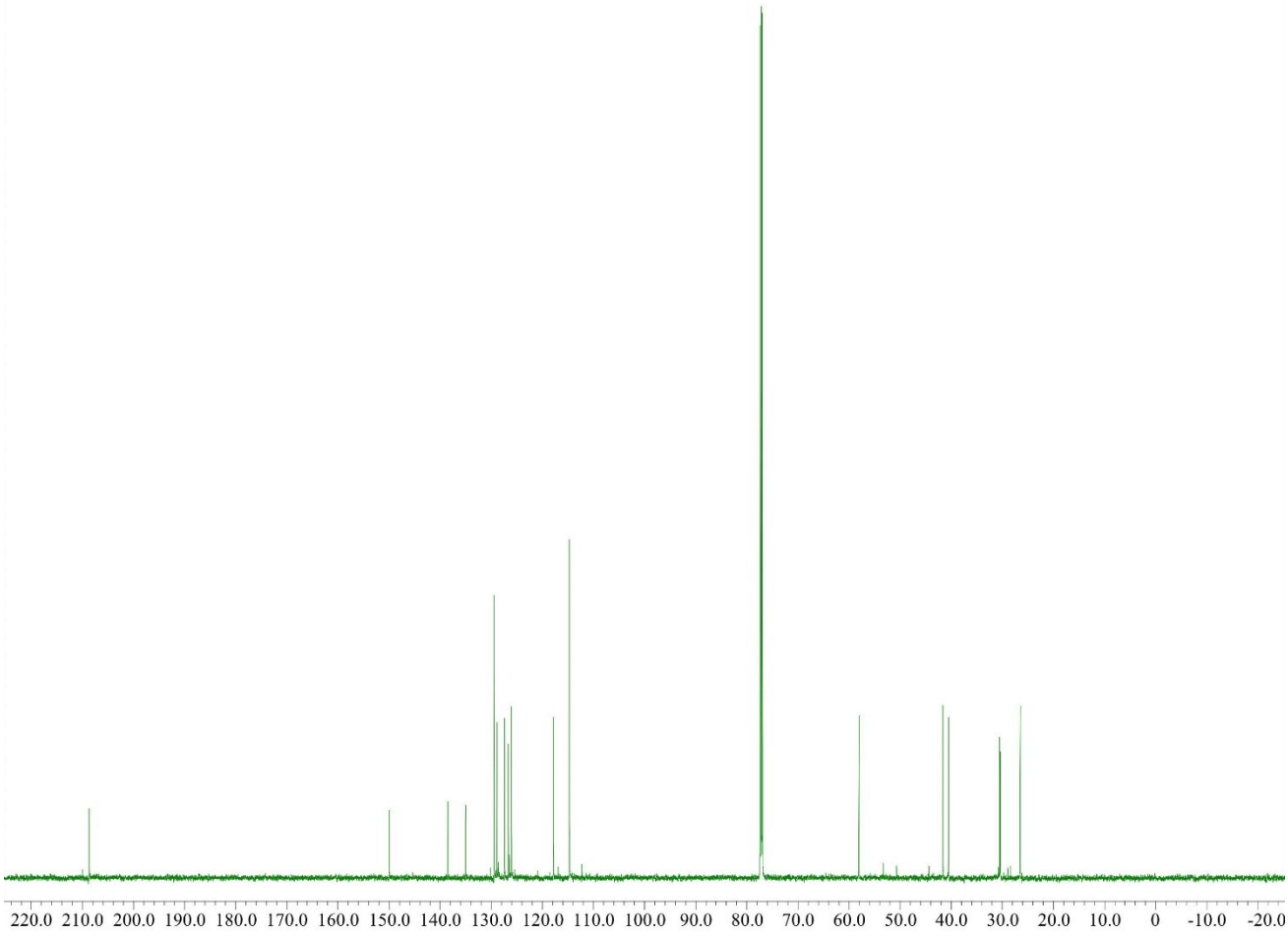
220.0 210.0 200.0 190.0 180.0 170.0 160.0 150.0 140.0 130.0 120.0 110.0 100.0 90.0 80.0 70.0 60.0 50.0 40.0 30.0 20.0 10.0 0 -10.0 -20.0

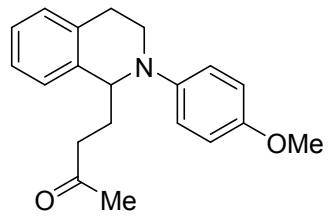
N
OMe
O
Me

6b

10.0
9.0
8.0
7.0
6.0
5.0
4.0
3.0
2.0
1.0
0

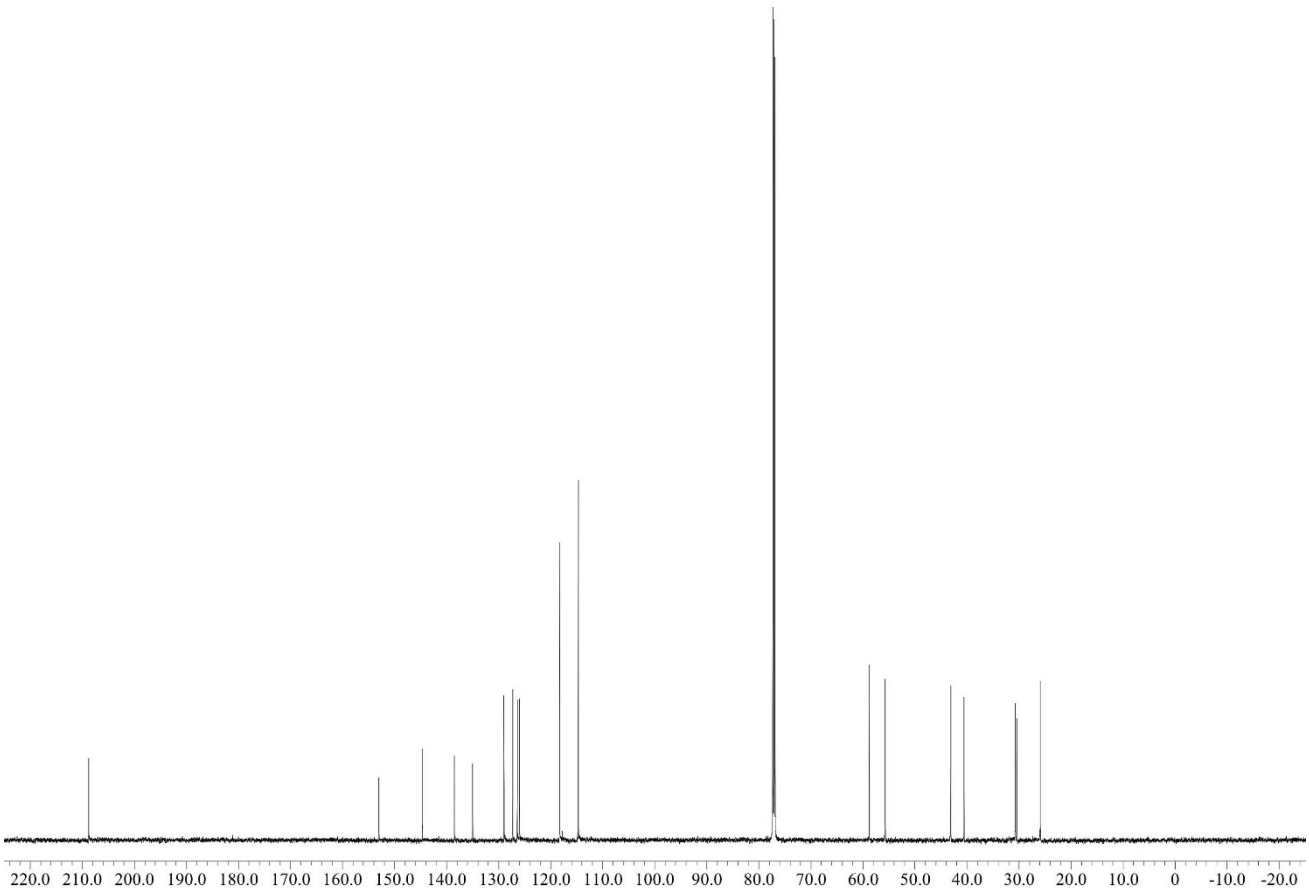
220.0 210.0 200.0 190.0 180.0 170.0 160.0 150.0 140.0 130.0 120.0 110.0 100.0 90.0 80.0 70.0 60.0 50.0 40.0 30.0 20.0 10.0 0 -10.0 -20.0

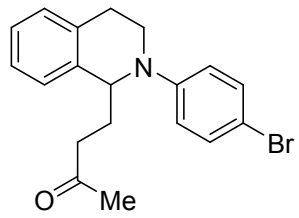
N
Br
O
Me

6c

10.0
9.0
8.0
7.0
6.0
5.0
4.0
3.0
2.0
1.0
0

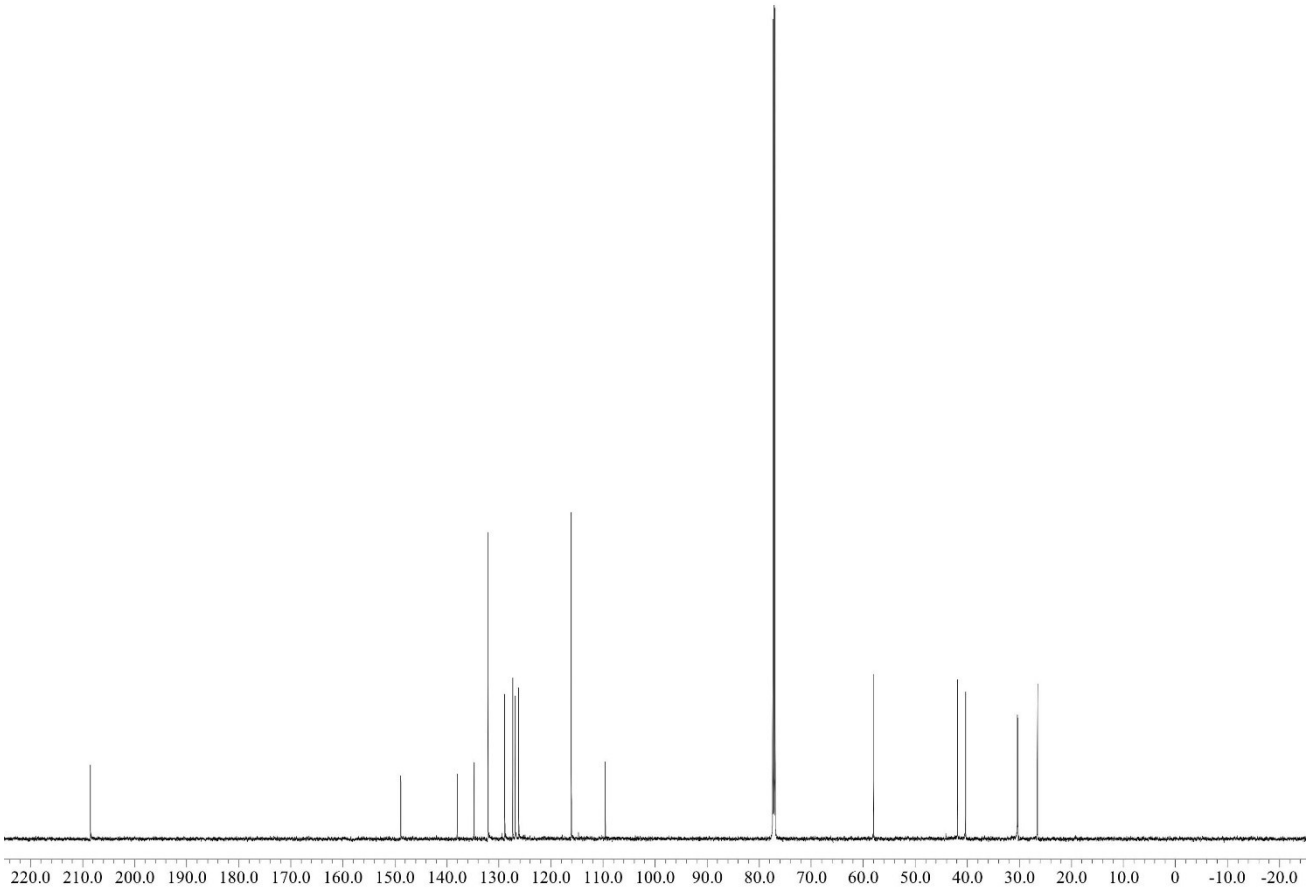
220.0 210.0 200.0 190.0 180.0 170.0 160.0 150.0 140.0 130.0 120.0 110.0 100.0 90.0 80.0 70.0 60.0 50.0 40.0 30.0 20.0 10.0 0 -10.0 -20.0

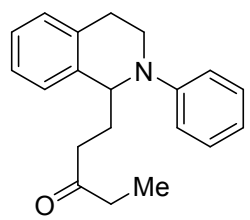
N
O
Me

6e

10.0
9.0
8.0
7.0
6.0
5.0
4.0
3.0
2.0
1.0
0

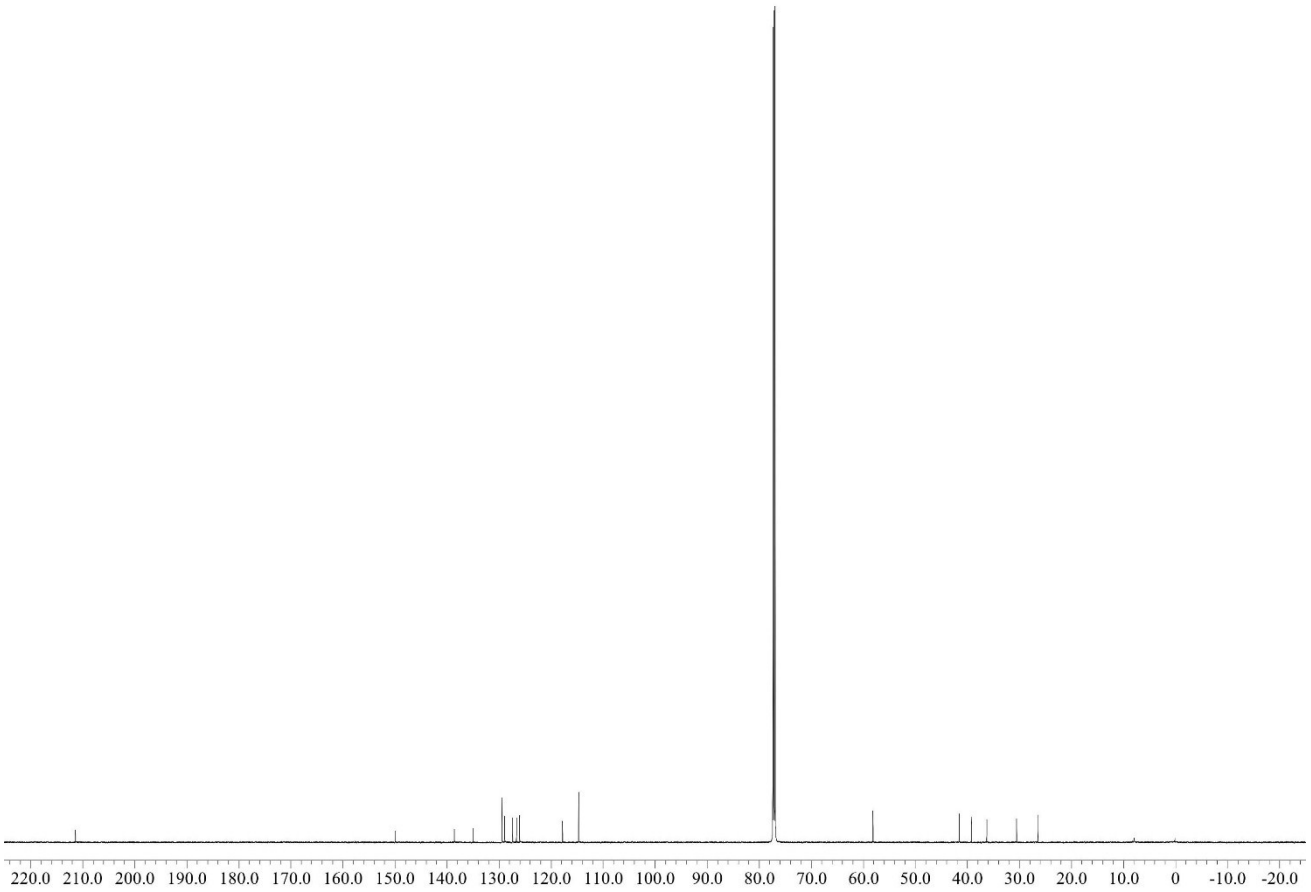
220.0 210.0 200.0 190.0 180.0 170.0 160.0 150.0 140.0 130.0 120.0 110.0 100.0 90.0 80.0 70.0 60.0 50.0 40.0 30.0 20.0 10.0 0 -10.0 -20.0

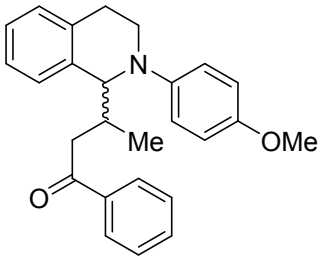

6f
major diastereomer

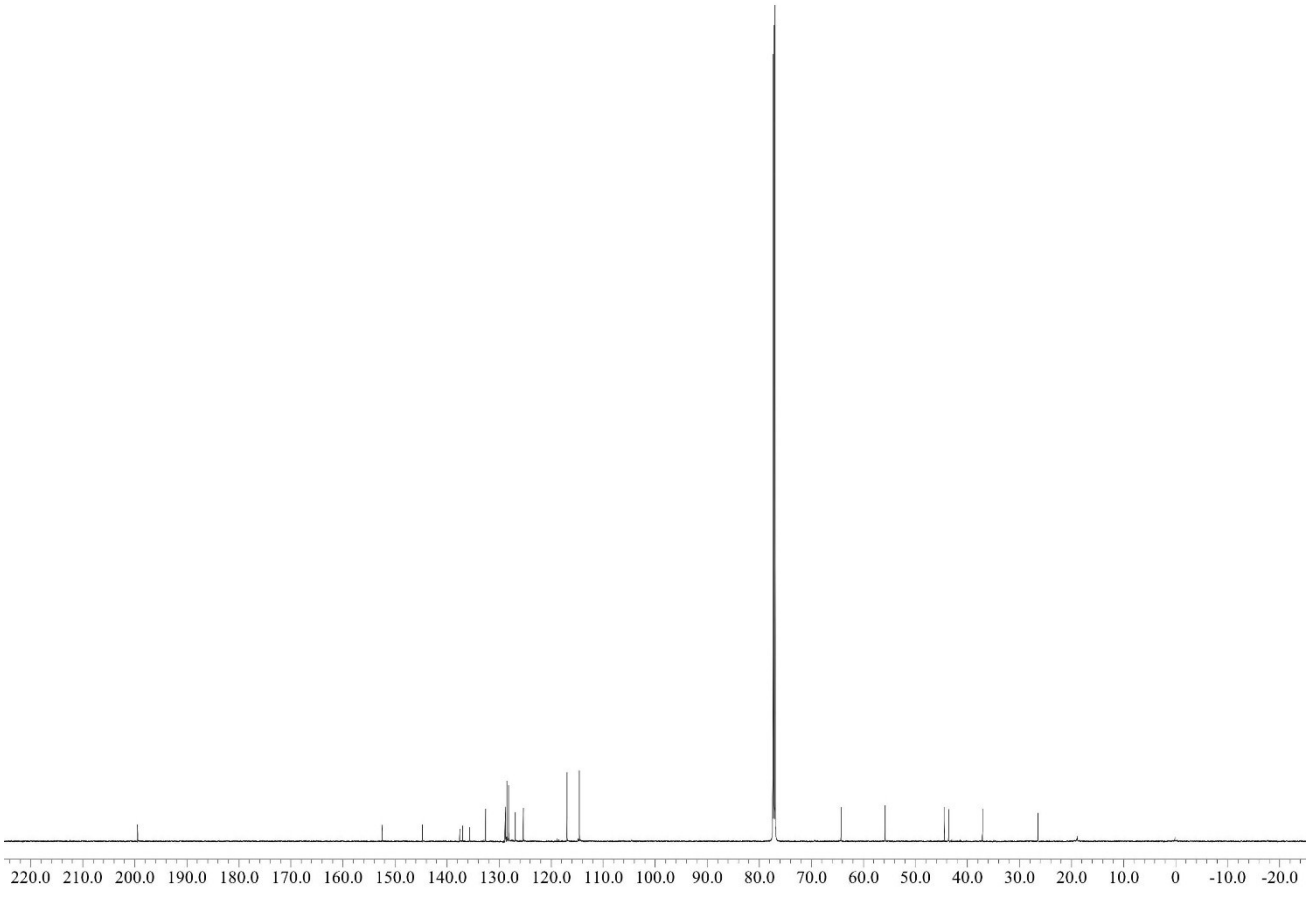

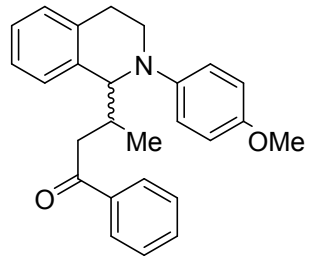

6f
minor diastereomer